Brain, Behavior, and Immunity 101 (2022) 231–245

Contents lists available at ScienceDirect

Brain Behavior and Immunity

journal homepage: www.elsevier.com/locate/ybrbi

Chronic IL-10 overproduction disrupts microglia-neuron dialogue similar to aging, resulting in impaired hippocampal neurogenesis and spatial memory

Paula Sanchez-Molina [a,b,*,1], Beatriz Almolda [a,b,1], Lydia Giménez-Llort [a,c], Berta González [a,b], Bernardo Castellano [a,b]

[a] Institute of Neurosciences. Universitat Autònoma de Barcelona, 08193 Bellaterra, Barcelona, Spain
[b] Department of Cell Biology, Physiology and Immunology, School of Medicine, Universitat Autònoma de Barcelona, 08193 Bellaterra, Barcelona, Spain
[c] Department of Psychiatry and Forensic Medicine, School of Medicine, Universitat Autònoma de Barcelona, 08193 Bellaterra, Barcelona, Spain

ARTICLE INFO

Keywords:
Neurogenesis
IL-10
Aging
Microglia
Memory
CX3CR1
CD200R
Hippocampus

ABSTRACT

The subgranular zone of the dentate gyrus is an adult neurogenic niche where new neurons are continuously generated. A dramatic hippocampal neurogenesis decline occurs with increasing age, contributing to cognitive deficits. The process of neurogenesis is intimately regulated by the microenvironment, with inflammation being considered a strong negative factor for this process. Thus, we hypothesize that the reduction of new neurons in the aged brain could be attributed to the age-related microenvironmental changes towards a pro-inflammatory status. In this work, we evaluated whether an anti-inflammatory microenvironment could counteract the negative effect of age on promoting new hippocampal neurons. Surprisingly, our results show that transgenic animals chronically overexpressing IL-10 by astrocytes present a decreased hippocampal neurogenesis in adulthood. This results from an impairment in the survival of neural newborn cells without differences in cell proliferation. In parallel, hippocampal-dependent spatial learning and memory processes were affected by IL-10 overproduction as assessed by the Morris water maze test. Microglial cells, which are key players in the neurogenesis process, presented a different phenotype in transgenic animals characterized by high activation together with alterations in receptors involved in neuronal communication, such as CD200R and CX3CR1. Interestingly, the changes described in adult transgenic animals were similar to those observed by the effect of normal aging. Thus, our data suggest that chronic IL-10 overproduction mimics the physiological age-related disruption of the microglia-neuron dialogue, resulting in hippocampal neurogenesis decrease and spatial memory impairment.

1. Introduction

Neurogenesis is the process of new cell formation from neural stem/progenitor cells (NSCs), which have the ability to proliferate and differentiate into astrocytes, oligodendrocytes, or neurons (Akkermann et al., 2017; Bond et al., 2020; Hirabayashi and Gotoh, 2005; Mira and Morante, 2020; Taupin and Gage, 2002). After the nervous system development in the embryonic stage, neurogenesis remains physiologically active in specific cerebral regions of mammals (Altman and Das, 1965; Eriksson et al., 1998; Kaplan and Hinds, 1977). Specifically, two neurogenic niches have been described in the adult mammal brain: the subventricular zone (SVZ) of the lateral ventricles and the subgranular zone (SGZ) of the hippocampal dentate gyrus (Imayoshi et al., 2009; Ming and Song, 2005).

The newborn neurons formed in the SGZ during adulthood migrate through the granular cell layer of the dentate gyrus and are integrated into the existing neuronal circuits participating in hippocampal-dependent memories (Saxe et al., 2006; Snyder et al., 2005; Stanfield and Trice, 1988). However, the type of memory in which new hippocampal neurons are involved is controversial (Deng et al., 2010). Despite the fact that quantifying the behavioral relevance of hippocampal neurogenesis in rodents is challenging (Lazic et al., 2014), there is a consensus of its significant influence on cognition (pattern separation and cognitive flexibility) and mood (anxiety- and depressive-like behaviors) (Anacker and Hen, 2017; Forte et al., 2021). During aging, a dramatic decrease of NSCs proliferation, leading to reduced

* Corresponding author at: Unitat d'Histologia, Facultat de Medicina, Universitat Autònoma de Barcelona, 08193 Bellaterra, Barcelona, Spain.
E-mail address: paula.sanchez@uab.cat (P. Sanchez-Molina).
[1] These authors contributed equally to this work.

https://doi.org/10.1016/j.bbi.2021.12.026
Received 1 June 2021; Received in revised form 24 December 2021; Accepted 29 December 2021
Available online 3 January 2022

neurogenesis, is specifically observed in the dentate gyrus (Bondolfi et al., 2004; Kuhn et al., 1996; Kuipers et al., 2015) concomitant with age-related cognitive deficits (Drapeau et al., 2003; Van Praag et al., 2005; Villeda et al., 2011).

The systemic and the local microenvironment is one of the main factors that regulate adult neurogenesis (Borsini et al., 2015; Carpentier and Palmer, 2009; Palmer et al., 2000; Villeda et al., 2011). In the aged hippocampus, the microenvironment is altered towards a pro-inflammatory and oxidized status (Cornejo and von Bernhardi, 2016; Lucin and Wyss-Coray, 2009; Ojo et al., 2015). Numerous studies demonstrate that inflammation is detrimental to the process of neurogenesis (Carpentier and Palmer, 2009; Ekdahl et al., 2003; Monje et al., 2003). Thus, induction of pro-inflammatory molecules, such as IL-6 (Monje et al., 2003; Vallières et al., 2002), IL-1β (Goshen et al., 2008; Hueston et al. 2018; Koo and Duman, 2008; Ryan et al., 2013), TNF-α (Cacci et al., 2005; Sheng et al., 2005) and nitric oxide (Packer et al., 2003), has an inhibitory effect on the generation of new hippocampal neurons. Contrary to pro-inflammatory signaling, little is known about the influence of anti-inflammatory molecules on neurogenesis. However, some studies have demonstrated that growth factors (Battista et al., 2006; Lichtenwalner et al., 2001; Scharfman et al., 2005; Wagner et al., 1999; Zigova et al., 1998) and anti-inflammatory cytokines (Butovsky et al., 2006; Kiyota et al., 2010; Kiyota et al., 2012) promote neurogenesis.

In this context, microglial cells play an important role in regulating neuroinflammation and, therefore, neurogenesis. Accordingly, it has been demonstrated that a pro-inflammatory microglial activation impacts negatively on the hippocampal neurogenesis by the secretion of pro-inflammatory cytokines (Cacci et al., 2005; Carpentier and Palmer, 2009; Monje et al., 2003; Nakanishi et al., 2007). In agreement, Ekdahl and collaborators showed a significant negative correlation between the number of LPS-activated microglia and the number of newborn neurons in the hippocampal neurogenic niche (Ekdahl et al., 2003). The importance of microglia-neuron communication in both neurogenesis and aging must also be highlighted. In this sense, alterations in the "do-not-eat-me" signaling, which maintains microglial cells in a homeostatic state, impact the generation of new neurons (Bachstetter et al., 2011; Varnum et al., 2015; Vukovic et al., 2012). In addition to microglial cells, other immune cells, such as lymphocytes, can modulate neurogenesis (Aharoni et al., 2005; Wolf et al., 2009).

Because most of the studies exploring the influence of the neurogenic microenvironment have been performed *in vitro* or by acute administration of specific molecules, it is of special interest to study the effect of a local and chronic microenvironment under physiological conditions *in vivo*. In this regard, Hueston et al. showed that long-term overexpression of the pro-inflammatory cytokine IL-1β reduces hippocampal neurogenesis and impairs pattern separation behavior in adult rats (Hueston et al. 2018), whereas in adolescent rats this reduction was independent of cognitive performance (Pawley et al. 2020). Specifically, the anti-inflammatory cytokine IL-10 has been described to influence neurogenesis differently *in vivo* depending on the administration route and the neurogenic niche. Thus, hippocampal IL-10 gene delivery by adeno-associated viruses enhances neurogenesis and spatial cognitive function, as shown by better memory acquisition and recall in a two-day radial water maze, in the APP + PS1 Alzheimer's disease mouse model (Kiyota et al., 2012), whereas intraventricular IL-10 administration in WT mice reduces neurogenesis of the SVZ (Perez-Asensio et al., 2013). Of special interest are previous results from our research group describing neuronal and microglial modifications in the hippocampus of adult and aged mice with astrocyte-targeted overproduction of IL-10 (Almolda et al., 2015; Sanchez-Molina et al., 2021). Considering the direct association between higher inflammation and lower neurogenesis in aging, the present study aims to evaluate the impact that an anti-inflammatory microenvironment produced by chronic astrocyte-targeted IL-10 overproduction exerts on the hippocampal neurogenesis and behavior in adult and aged mice under physiological conditions.

2. Material and methods

2.1. Animals

Transgenic mice with astrocyte-targeted overproduction of IL-10 (GFAP-IL10Tg) and their corresponding wild-type (WT) littermates were used in this study ($n = 111$). The experimental groups used in this study are indicated in Table 1. GFAP-IL10Tg mouse generation on the C57BL/6 background was previously described (Almolda et al., 2015). Genotype determination was performed by polymerase chain reaction (PCR) analysis of DNA obtained from mice-tail biopsies. Animals of both sexes were distributed into two experimental groups according to age: adult (4–6 months old) and aged (18–24 months old) mice. Animals were maintained in standard cages with food and water *ad libitum,* in a 12 h light/dark cycle (lights on at 8 a.m.), 22 °C ± 2 °C and 50%-60% humidity. All experimental animal work was conducted according to Spanish regulations (Ley 32/2007, Real Decreto 1201/2005, Ley 9/2003 and Real Decreto 178/2004) in agreement with the EU Directive (2010/63/UE) on this subject. The study complies with the ARRIVE guidelines developed by the NC3Rs and aims to reduce the number of animals used.

2.2. Behavioral assessment

A set of four behavioral tests was used as previously described (Giménez-Llort et al., 2010; Giménez-Llort et al., 2021) to characterize anxiety-like behavior, spatial memory and cognitive flexibility, which are related with hippocampal neurogenesis (Dupret et al., 2008; Garthe et al., 2009; Kee et al., 2007; Revest et al., 2009), in adult (4–5 months old) and aged (18–19 months old) mice of both genotypes ($n = 7$–12 per experimental group). Physical status and animal survival were also evaluated.

Corner test: Neophobia in a new standard home-cage was measured as the number of visited corners and rearings during 30 s.

Open field test: Animals were placed in the center of a white apparatus (48 cm × 33 cm × 25 cm) and observed for 5 min. Vertical activity was manually quantified in mice, counting the rearing latency and the number of rearings for each minute of the test. Horizontal activity, including total distance traveled, total time in movement, and the time in the apparatus center/periphery, was analyzed in mice using the ANY-maze behavioral tracking system. Latency, number, and duration of grooming episodes, as well as the number of defecations and urinations, were also recorded to measure emotionality.

T-maze: Animals were placed (facing the wall) at the beginning of the vertical arm of a T-shaped black maze (short arms of 30 cm), a mild anxiogenic environment resembling burrows. Spontaneous alternation behavior was observed during 3 min. The time to reach the three-arms intersection (nose criteria) and the number of errors (exploration of an already explored arm) were manually recorded to assess the animals coping-with-stress capacity and their working memory, respectively.

Morris water maze: Hippocampal-dependent spatial short- and long-term learning and memory were analyzed for five consecutive days using three paradigms consisting of one day of visual-perceptual (cue) learning task, followed by four days of reversal place-learning task demanding cognitive flexibility, and a final probe trial for short-term memory (Fig. 4A-C). The test was carried out in a circular pool (120-cm diameter, 60-cm height) with opaque white water at 25 °C and surrounded by black curtains. On the first day, a cue-learning task with a flag in a visible platform (7-cm diameter) was performed (four trials of 1 min maximum, 60 min intertrial time), and escape latencies to reach the platform were recorded. The following four days, a reversal place-learning paradigm (four trials of 1 min maximum, 60 min intertrial time) with the platform hidden 1 cm below the water surface and external cues in the black walls was performed and escape latencies to reach the platform were also recorded. In both paradigms, the animals were introduced into the pool by a different cardinal point per trial. Mice

Table 1
Experimental groups used in the study.

	Behavioral and biochemical analysis		BrdU administration and histological analysis		Flow cytometry analysis	
	4–6 months (n = 17)	18–21 months (n = 24)	4–5 months (n = 23)	19–20 months (n = 17)	5–6 months (n = 16)	23–24 months (n = 14)
WT (n = 55)	7	12	12	9	8	7
GFAP-IL10Tg (n = 56)	10	12	11	8	8	7

that failed to find the platform within the 60 s were manually guided and placed on it for 10 s -as the successful animals- before taking them out of the pool. On the fifth day, two hours after the last place-learning trial, the platform was removed and a probe was performed recording the mice's trajectory in the pool for 1 min. The time the mouse spent swimming in the quadrant where the platform was previously located was used as an indicator of memory. The ANY-maze behavioral tracking system was used to record and analyze the trajectories of this test.

2.3. BrdU administration

5-Bromo-2′-deoxyuridine (BrdU), a synthetic thymidine analog, was used to study neural stem cell proliferation because it is incorporated into DNA during the S-phase cell cycle. One 100 mg/kg dose of BrdU (B5002, Sigma-Aldrich) diluted in NaCl (pH 7.4) was intraperitoneally injected during five consecutive days in adult (5 months old) and aged (19 months old) mice of both genotypes. A set of animals (n = 3–5 per experimental group) was euthanized one day after the last BrdU administration to evaluate cell proliferation, whereas another set of animals (n = 4–8 per experimental group) was euthanized two weeks after the last BrdU administration, following the protocol described in Kuipers et al. (2015), to evaluate cell survival (Fig. 1F).

2.4. Tissue processing for histological analysis

Under an intraperitoneal anesthetic solution of xylazine (30 mg/kg) and ketamine (120 mg/kg), mice were intracardially perfused for 10 min with 4% paraformaldehyde in 0.1 M phosphate buffer (pH 7.4). The brains were quickly removed, post-fixed for 4 h at 4 °C in the same fixative solution, cryoprotected with 30% sucrose in 0.1 M phosphate buffer for 48 h at 4 °C, frozen in ice-cold 2-methylbutane (320404, Sigma-Aldrich) and stored at −80 °C. Parallel coronal sections (30-μm-thick) of the telencephalon containing the hippocampus were obtained using a CM 3050S Leica cryostat and were stored at −20 °C in an anti-freeze solution containing 20% sucrose, 30% ethylene glycol and 1% polyvinylpyrrolidone until use.

2.5. Single immunohistochemistry

For the visualization of neuroblasts and proliferating cells, brain sections were immunostained with antibodies against doublecortin (DCX) and BrdU, respectively, in adult (4–5 months old) and aged (19–20 months old) mice of both genotypes. Frozen free-floating sections were washed in Tris-buffered saline (TBS; 0.05 M, pH 7.4) to eliminate the anti-freeze solution and incubated for 10 min with 2% H_2O_2 and 70% methanol in distilled H_2O to inhibit endogenous peroxidase. For BrdU immunostaining, DNA denaturation incubating the sections in 0.082 N HCl at 4 °C for 10 min followed by another incubation in 0.82 N HCl at 37 °C for 30 min was performed. Sections were then neutralized with 0.1 M sodium borate (pH 8.5). After washes with TBS containing 1% Triton X-100 (TBS-T; 0.05 M, pH 7.4), all sections were incubated for 1 h at room temperature (RT) in a blocking buffer (BB) containing 10% fetal bovine serum (FBS) in TBS-T. Afterwards, sections were incubated overnight at 4 °C plus 1 h at RT with anti-DCX (1:1000; ab77450, Abcam) or anti-BrdU (1:100; ab6326, Abcam) primary antibodies diluted in BB. Neonatal brain sections were used as positive control for DCX, whereas the corresponding small intestine sections of animals treated with BrdU were used as positive control for BrdU. Sections incubated in BB lacking the primary antibody were used as negative control. After washes with TBS-T, sections were incubated for 1 h at RT with biotinylated anti-rabbit (1:500; BA-1000, Vector Laboratories) and anti-rat (1:500; BA-4001, Vector Laboratories) secondary antibodies diluted in BB for DCX and BrdU immunostaining, respectively. Following this, sections were washed with TBS-T and incubated for 1 h at RT with horseradish peroxidase (HRP)-conjugated streptavidin (1:500; SA-5004, Vector Laboratories). After washes with TBS and Tris Buffer (TB; 0.05 M, pH 7.4), the immunolabeling was visualized incubating the sections for 3 min with a 3,3′-diaminobenzidine (DAB) Substrate Kit (SK-4100, Vector Laboratories) following the manufacturer's instructions. In this step, nickel was additionally added for the visualization of BrdU. Afterwards, sections were washed in TB, mounted onto gelatinized slides and air-dried at RT. To provide cytological details of DCX immunostaining, sections were counter-stained with 0.1% toluidine blue diluted in Walpole's buffer (0.05 M, pH 4.5). Finally, sections were dehydrated in graded alcohols, washed in N-butyl alcohol in the case of toluidine staining, immersed in xylene and coverslipped with dibutylphthalate polystyrene xylene (DPX) mounting medium.

2.6. Double immunofluorescence

To evaluate whether proliferating cells express IL-10 receptor (IL-10R), double immunolabeling against BrdU and IL-10R markers was performed in animals sacrificed one day after the last BrdU administration. A double immunofluorescence against IL-10R and GFAP was also performed. Frozen free-floating brain sections were washed in TBS and DNA denaturation was performed as is explained in the above section for BrdU immunostaining. After washes with TBS-T, brain sections were incubated for 1 h at RT in a BB containing 10% FBS in TBS-T followed by anti-BrdU primary antibody (1:100; ab6326, Abcam) or anti-GFAP primary antibody (1:6000; G3893, Sigma-Aldrich) diluted in the BB, overnight at 4 °C and 1 h at RT. After washes with TBS-T, sections were incubated for 1 h at RT with an anti-rat AlexaFluor-488 conjugated secondary antibody (1:1000; A-11006, Thermo Fisher) or an anti-mouse AlexaFluor-488 conjugated secondary antibody (1:1000; A-11029, Thermo Fisher) diluted in BB. Following another blocking incubation for 1 h at RT, sections were incubated with anti-IL-10RA primary antibody (1:100; ab225820, Abcam) diluted in the BB for 48 h at 4 °C and 1 h at RT. Then, incubations for 1 h at RT with biotinylated anti-rabbit secondary antibody (1:500; BA-1000, Vector Laboratories), followed by incubation with AlexaFluor-555 conjugated streptavidin (1:1000; S32355, Thermo Fisher), were performed. After washes with TBS-T and TBS, sections were incubated with 4,9,6-diamidino-2-phenylindole (DAPI) (1:10000; D9542, Sigma-Aldrich) in TB for 5 min at RT to stain the cell nuclei. Finally, sections were washed with TB, mounted on slides and coverslipped with Fluoromount (0100–01, SouthernBiotech) mounting medium. Representative photos in the dentate gyrus were captured at 63x magnification using a Zeiss LSM700 confocal microscope.

2.7. Cell quantification

Photographs were captured with a DXM 1200F Nikon digital camera mounted on a brightfield Nikon Eclipse 80i microscope using the ACT-1

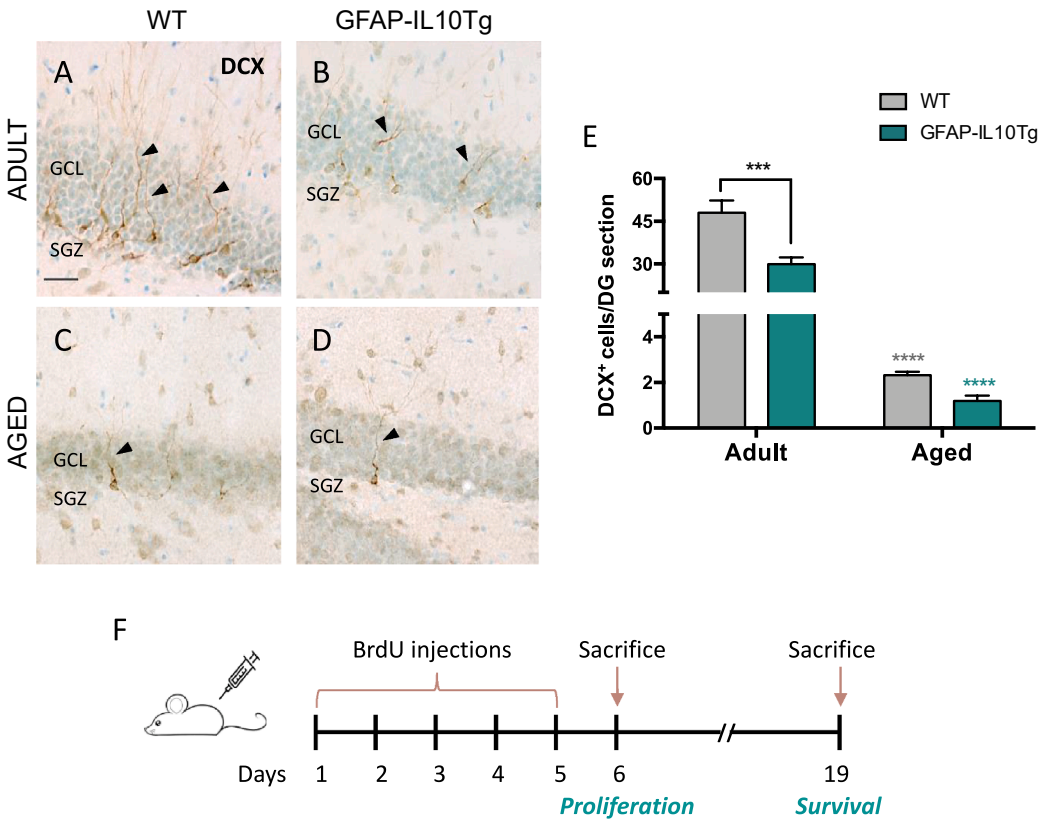

(caption on next page)

Fig. 1. Hippocampal neurogenesis is decreased in GFAP-IL10Tg mice due to low survival of neural proliferating cells. Representative images showing doublecortin (DCX) immunostaining in the granular cell layer of WT (A, C) and GFAP-IL10Tg (B, D) mice during adulthood (A, B) and aging (C, D). Quantification of DCX^+ cells per dentate gyrus (DG) section is represented in the graph (E). Temporal scheme of intraperitoneal BrdU administration (5 consecutive days) and time points of mice sacrifice (days 6 and 19) is shown in the panel (F). Graphs showing the number of proliferating $BrdU^+$ cells (G) and surviving $BrdU^+$ cells (H) per dentate gyrus section. Representative images showing BrdU immunostaining in the dentate gyrus after two weeks of the last BrdU administration (survival time) in adult WT (I) and GFAP-IL10Tg (J) mice. Representative images showing BrdU and IL-10 receptor (IL-10R) double immunostaining in the dentate gyrus after one day of the last BrdU administration in adult WT (K) and GFAP-IL10Tg (L) mice. Statistical analysis was performed by two-way ANOVA followed by Tukey's post hoc tests. Grey and cyan asterisks refer to significant differences by age in WT and GFAP-IL10Tg mice, respectively. $*p < 0.05$, $**p < 0.01$, $***p < 0.001$, $****p < 0.0001$. Data are represented as the mean ± SEM. Abbreviations: DCX; doublecortin, BrdU; 5-Bromo-2′-deoxyuridine, DG; dentate gyrus, GCL; granular cell layer, SGZ; subgranular zone, IL-10R; IL-10 receptor. Arrow heads indicate dendrites on neuroblasts. (For interpretation of the references to colour in this figure legend, the reader is referred to the web version of this article.)

2.20 software (Nikon Corporation). A minimum of four animals of each age group was analyzed using the sections immunostained for DCX and BrdU. For each animal, at least 6 dentate gyrus areas from hippocampal sections separated from each other by 300 μm were used to manually count the number of DCX^+ cells in the granular cell layer using 40x magnification. $BrdU^+$ cells were quantified manually in the granular cell layer and the hilus region from at least 12 hippocampal dentate gyrus sections at 40x magnification.

2.8. Blood collection

Under an anesthetic solution of xylazine (30 mg/kg) and ketamine (120 mg/kg), blood from adult (6 months old) and aged (21 months old) mice was intracardially extracted from the right ventricle and centrifuged at 9,300 × *g* for 5 min at 4 °C. Serum was then collected and stored at −80 °C until use.

2.9. Tissue processing for biochemical analysis

Under an intraperitoneal anesthetic solution of xylazine (30 mg/kg) and ketamine (120 mg/kg), mice were intracardially perfused with cold 0.1 M Phosphate-Buffered Saline (PBS) at pH 7.4 for 1 min. The hippocampus was quickly dissected, frozen in liquid nitrogen and stored at −80 °C. Tissue was homogenized using a polytron homogenizer in a lysis buffer containing 25 mM HEPES at pH 7.4 (H3375, Sigma-Aldrich), 0.2% IGEPAL (I-3021, Sigma-Aldrich), 5 mM $MgCl_2$ (A376433, Merck), 1.3 mM EDTA at pH 8 (20302, VWR), 1 mM EGTA at pH 8 (E4378, Sigma-Aldrich), 1 mM PMSF (P7626, Sigma-Aldrich), protease inhibitor cocktail (1:100; P8343, Sigma-Aldrich) and phosphatase inhibitor cocktail (1:100; P0044, Sigma-Aldrich) in deionized water. After 2 h at 4 °C, tissue lysates were centrifuged at 15,600 × *g* for 5 min at 4 °C. Then, the supernatants were collected and stored as aliquots at −80 °C until use. In all of the study, the hippocampus of each animal was analyzed separately.

2.10. Luminex bead-based multiplex assay

Total protein concentration of each hippocampal lysate was determined with a commercial Pierce BCA Protein Assay Kit (23225, Thermo Scientific) according to the manufacturer's instructions. To quantify specific proteins, Luminex® Multiple Analyte Profiling (xMAP®) technology was used. In adult (6 months old) and aged (21 months old) animals of both genotypes, IL-10, IL-6, IL-1β and TNF-α cytokines levels were measured by MILLIPLEX® $_{MAP}$ Kit (MCYTOMAG-70 K, Merck) in hippocampal ($n = 6$–9 per experimental group) and serum ($n = 4$–5 per experimental group) samples. In the same animals, hippocampal levels of brain-derived neurotrophic factor (BDNF) and fractalkine (CX3CL1) were measured by MILLIPLEX® $_{MAP}$ Kit (MMYOMAG-74 K, Merck). Both Luminex multiplex assays were performed according to the manufacturer's protocol. Briefly, 25 μL of each sample (total protein concentration of 3 μg/μL), standards or controls were added to their corresponding wells in a 96-well plate. Additionally, 25 μL of Assay Buffer were added to samples' wells, whereas 25 μL of lysis buffer (See "2.9. Tissue processing for biochemical analysis" section) were added to standard and control wells. In all wells, 25 μL of magnetic beads conjugated with the antibodies of interest were added and incubated on a plate-shaker overnight at 4 °C. After removing wells' content with a handheld magnet and two washes with Wash Buffer, 25 μL of Detection Antibodies were added to each well and incubated with agitation for 1 h at RT. Next, 25 μL of Streptavidin-Phycoerythrin were also added to each well and incubated with agitation for 30 min at RT. Finally, the wells were washed twice with Wash Buffer and 150 μL of Drive Fluid were added, followed by a 5-min shaking. The Luminex MAGPIX® instrument with xPONENT® 4.2 software was used to read and analyze the plate.

2.11. Enzyme-linked immunosorbent assay (ELISA)

Hippocampal transforming growth factor-β (TGFβ) levels in adult (6 months old) and aged (21 months old) animals of both genotypes ($n = 4$–5 per experimental group) were quantified using a mouse TGFβ1 uncoated ELISA kit (88-8350, Invitrogen) according to the manufacturer's instructions. Briefly, a 96-well plate was coated overnight at 4 °C with Capture Antibody in Coating Buffer. After washes, wells were blocked with ELISA/ELISASPOT Diluent for 1 h at RT. Followed by washes, 100 μL of standards and samples (total protein concentration of 4 μg/μL), previously treated with 1 N HCl for 10 min at RT and 1 N NaOH, were incubated overnight at 4 °C in separate wells. Next, Detection Antibody was added to the wells and incubated for 1 h at RT. Afterwards, Avidin-HRP was incubated for 30 min at RT. Finally, TMB Solution was incubated for 15 min at RT followed by addition of 2 N H_2SO_4. Immediately after, plate was read at 450 nm in a microplate reader and data were expressed as pg/mL of protein.

2.12. Flow cytometry

Characterization of microglial and neuronal populations was performed by flow cytometry. Under an intraperitoneal anesthetic solution of xylazine (30 mg/kg) and ketamine (120 mg/kg), adult (5–6 months old) and aged (23–24 months old) animals of both genotypes ($n = 7$–8 per experimental group) were intracardially perfused with cold 0.1 M PBS at pH 7.4 for 1 min. Hippocampi were quickly dissected and dissociated with a 160-μm nylon mesh in Hank's Balanced Salt Solution (HBSS) with 10% FBS and were then passed into a centrifuge tube through a 70-μm cell strainer. The splenocyte cell suspension obtained from one animal was used as positive control throughout the procedure. After three centrifugations for 10 min at 310 × *g* (24 °C) retaining the pellet, the homogenized tissue was digested in a solution composed of 1.25% deoxyribonuclease I (D5025, Sigma-Aldrich) and 0.5% collagenase IV (17104019, Thermo Fisher) in HBSS for 30 min at 37 °C. Cellular suspensions were centrifuged for 10 min at 310 × *g* (24 °C), then a density gradient was generated by using 1.122 g/mL and 1.088 g/mL of Percoll® (GE17-0891–02, Sigma-Aldrich) and centrifuging for 20 min at 600 × *g* (24 °C) with the rotor deceleration set to its minimum value. The upper phase corresponding to myelin was removed, and the intermediate phase containing cells was collected. Cellular suspensions were centrifuged for 5 min at 860 × *g*, and 200 μL of each sample diluted in PBS with 2% FBS were seeded in a 96-well conical bottom plate. Each

sample was divided into five wells, attending to the following treatments: microglial primary antibodies combination, neuronal primary antibodies combination, microglial isotypes control combination, neuronal isotypes control combination and unstained samples. After centrifugation for 4 min at 515 × *g* (4 °C), FcγIII (CD16) and FcγII (CD32) receptors expressed on cells were blocked adding 50 μL of CD16/32 antibody (1:250; 553142, BD Biosciences) diluted in PBS with 2% FBS to all of the wells for 20 min at 4 °C. After adding 150 μL of PBS with 2% FBS and centrifuging for 4 min at 515 × *g* (4 °C), surface markers of microglial cells and neurons were immunolabeled by incubating for 30 min at 4 °C in 50 μL of CD45-PerCP (1:400; 557235, BD Bioscience), CD11b-APC-Cy7 (1:400; 557657, BD Bioscience), CX3CR1-PE (1:400; FAB5825P, RD Systems), CD200R-AlexaFluor-647 (1:50; 566345, BD Bioscience), SIRPα-FITC (1:50; 144005, BioLegend), CD200-PE (1:400; 123807, BioLegend) and CD47-APC-Cy7 (1:50; 127525, BioLegend) antibodies diluted in PBS with 2% FBS. Samples in parallel wells were incubated with their corresponding conjugated-isotype control combinations (1:400; BD Biosciences). To immunolabel the intracellular marker NeuN, wells containing neuronal combinations of primary antibodies and isotype controls were treated with 200 μL of a Fixation/Permeabilization solution (00–5123-43 and 00–5223-56, eBioscience) for 40 min at 4 °C. After centrifugations with a 1X permeabilization buffer (00–8333-56, eBioscience) for 4 min at 515 × *g* (4 °C), 50 μL of biotinylated-NeuN antibody (1:400; MAB377B, Millipore) diluted in the permeabilization buffer were added to the corresponding wells and incubated for 30 min at 4 °C. Next, wells to study the neuronal combinations were incubated with Streptavidin-Cy5 (1:400; PA45001, Sigma-Aldrich) diluted in the permeabilization buffer for 20 min at 4 °C. After centrifugations, all samples were resuspended in 150 μL of PBS with 2% FBS and transferred from plate wells to cytometry tubes. Finally, 50 μL of CytoCount™ (S2366, Dako) fluorescent beads were added to the samples. Cell suspensions were acquired and read using a BD FACSCanto™ flow cytometer with BD FACSDiva™ software. Analysis of the data was performed using the FlowJo™ software.

2.13. Statistical analysis

Statistics and graphic representation were performed using the GraphPad Prism® software. To determine differences between the different groups of animals, two-way ANOVA followed by Tukey's *post hoc* test for multiple comparisons was used. p-value < 0.05 was considered statistically significant. All experimental results are expressed as mean ± SEM.

3. Results

3.1. Decreased hippocampal neurogenesis in mice overexpressing IL-10

To study net neurogenesis, the number of DCX positive cells, a specific marker of neuroblasts and immature neurons, was quantified in the granular cellular layer (GCL) of the dentate gyrus. In all experimental groups, DCX^+ cell bodies were found in the SGZ or the inner GCL (Fig. 1A-D). DCX^+ cells displayed the typical morphology of neuroblasts, extending dendrites from the GCL through to the molecular cell layer (Fig. 1A-D). Our results showed a dramatic decrease of DCX^+ cell numbers with aging regardless of genotype (Fig. 1E). Moreover, GFAP-IL10Tg mice presented a lower number of DCX^+ cells with respect to WT mice in adulthood (Fig. 1E). Indeed, two-way ANOVA showed main effects of age ($F(1, 16) = 192.90$, $p < 0.0001$), genotype ($F(1, 16) = 12.76$, $p < 0.01$) and interaction ($F(1, 16) = 9.94$, $p < 0.01$).

To determine whether the reduced neurogenesis observed in transgenic animals with respect to WT was due to a lower proliferation rate of NSCs, we visualized BrdU-labeled mitotic cells located in the SGZ one day after five consecutive days of BrdU administration. In the adult SGZ of the hippocampus, $BrdU^+$ cells were visualized in clusters, indicating recent mitotic divisions. In both genotypes, a significant reduction in the number of proliferating $BrdU^+$ cells was observed during aging (two-way ANOVA: age effect, $F(1, 12) = 48.83$, $p < 0.0001$) (Fig. 1G). However, no differences in the number of $BrdU^+$ cells were found between WT and GFAP-IL10Tg mice at any age in the proliferation period (Fig. 1G). The hippocampal hilus is another proliferating, but non neurogenic (Bondolfi et al., 2004), region of the adult CNS. In this area, a lower number of proliferating cells, as compared to the SGZ, was observed. As in the SGZ, the number of $BrdU^+$ cells in the hilus decrease with aging -although in a less pronounced way-, and no differences were detected between genotypes (data not shown).

Before NSC differentiation, some NSCs undergo apoptosis in a period taking approximately 15 days after their proliferation (Encinas et al., 2011; Sierra et al., 2010). Therefore, the next step we addressed was to analyze putative differences between WT and GFAP-IL10Tg animals in terms of NSC survival. Thus, following five days of consecutive BrdU injections, the number of surviving $BrdU^+$ cells was quantified two weeks after the last administration. At this time point, a slight reduction in the number of $BrdU^+$ cells, in comparing them with the number of $BrdU^+$ cells quantified one day after the last BrdU administration, was observed in adult WT mice (Fig. 1G,H). This reduction was significantly higher in adult GFAP-IL10Tg mice when compared to WT mice, showing that animals overexpressing IL-10 present a lower NSC survival rate in adulthood with respect to WT animals (Fig. 1H-J). In aging, these differences were attenuated by the general low number of proliferating NSCs (Fig. 1H). As for the number of DCX^+ cells, two-way ANOVA showed main effects of age ($F(1, 19) = 65.09$, $p < 0.0001$), genotype ($F(1, 19) = 11.24$, $p < 0.01$) and interaction ($F(1, 19) = 11.56$, $p < 0.01$) on the number of survival cells.

To determine whether IL-10 could be directly affecting NSC survival, we evaluated IL-10 receptor (IL-10R) expression in proliferating NSCs before their differentiation by a double immunofluorescence against BrdU and IL-10R. Our results demonstrated no expression of IL-10R in $BrdU^+$ cells of the SGZ (Fig. 1K,L). IL-10R expression was mainly observed in neuronal dendrites and astrocytes of the hippocampal CA area (data not shown), and in some neuronal bodies located in the hippocampal hilus. No variations in the expression pattern of IL-10R by age or genotype were observed.

3.2. Unaltered animal survival and physical status by IL-10 overexpression

No differences in survival between WT and GFAP-IL10Tg mice up to 24 months of age were observed. All animals reached the age of sacrifice without evidence of motor problems or physical deterioration. Body weight increased in WT and GFAP-IL10Tg mice upon aging without differences between genotypes (data not shown).

3.3. Neophobia and spatial memory impairment in GFAP-IL10Tg mice

Prior to cognition measurement, locomotion and anxiety-like behavior of mice were evaluated by the corner test and the open field test. As compared to adult WT mice, a lower number of visited corners was observed because of the effect of both age and genotype (two-way ANOVA: age effect, $F(1, 37) = 9.17$, $p < 0.01$; genotype effect, $F(1, 37) = 6.70$, $p < 0.05$; interaction effect, $F(1, 37) = 4.41$, $p < 0.05$) in the corner test for neophobia (Fig. 2A). In the open field test, this neophobia was also seen in aged GFAP-IL10Tg mice as a delayed rearing latency than in age-matched WT mice revealed by post-hoc analysis ($p = 0.05$) (Fig. 2B). However, the total vertical and horizontal locomotor activity recorded during the five min of the test was similar among all animal groups studied when considering rearings, distance traveled and time spent in the center of the open field, indicating no differences in total locomotion or anxiety-like behavior by age or genotype (Fig. 2C-F). Changes in emotionality were also found as indicated by a longer grooming latency in transgenic mice than in WT mice counterparts (two-way ANOVA: genotype effect, $F(1, 36) = 4.90$, $p < 0.05$) (Fig. 2G).

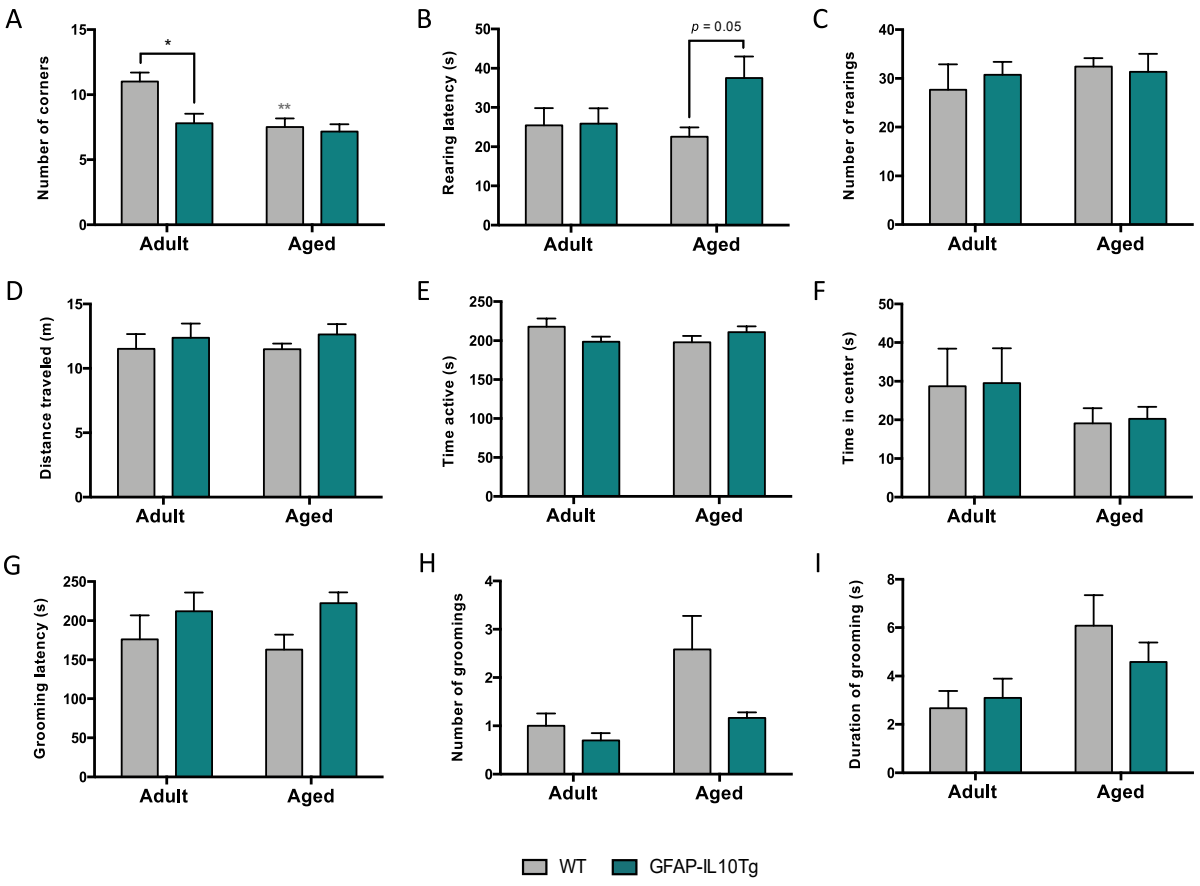

Fig. 2. GFAP-IL10Tg mice present increased neophobia, but normal total locomotion. Graph showing the number of visited corners in the corner test as measure of neophobia (A). In the open field test, vertical activity as measured by the rearing latency (B) and the number of total rearings (C). Horizontal activity is graphically represented by the distance traveled (D), the time active (E) and the time in the center of the apparatus (F). Quantification of grooming latency (G), total number of groomings (H) and total duration of grooming episodes (I) in the open field test. Statistical analysis was performed by two-way ANOVA followed by Tukey's post hoc tests. Grey asterisks refer to significant differences by age in WT mice. $^{*}p < 0.05$, $^{**}p < 0.01$. Data are represented as the mean ± SEM.

However, two-way ANOVA only showed age effect on the number ($F(1, 36) = 5.08$, $p < 0.05$) and the total duration ($F(1, 36) = 5.45$, $p < 0.05$) of grooming (Fig. 2H,I). In this test, no urination and a very low number of defecations were recorded in any of the groups studied.

Since neurogenesis of the dentate gyrus is involved in hippocampal-dependent memory, two spatial learning and memory tests, the T-maze and the Morris water maze, were used to evaluate possible cognitive deficits in working, short- and long-term learning and memory.

Working memory was assessed using the spontaneous alternation in the T-maze, where the number of arms-exploratory errors was quantified. In this memory task, the overall incidence of GFAP-IL10Tg mice making more than one single error (50%, 5/10 in adulthood, 6/12 in aging) was higher as compared to WT mice (18.75%, 1/6 in adulthood, 2/10 in aging), indicating working memory deficits (Fig. 3A). The latency to the arms intersection, which is related to coping with stress, showed a trend to be delayed with both aging and IL-10 overexpression albeit not reaching statistical significance (Fig. 3B).

For spatial short- and long-term learning and memory, three paradigms were used in the Morris water maze. On the first day, two-way ANOVA showed main effects of age ($F(1, 32) = 4.29$, $p < 0.05$) and

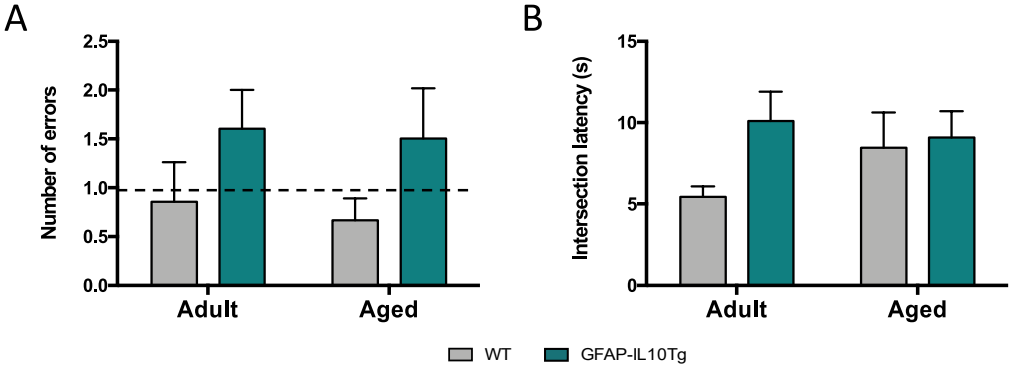

Fig. 3. Working memory deficits in GFAP-IL10Tg mice assessed by the spontaneous alternation in the T-maze. Graphs showing the number of errors that mice made by exploring the same arm again in the maze (A), and the latency to cross the intersection between vertical and horizontal arms (B) in WT and GFAP-IL10Tg mice. Statistical analysis was performed by two-way ANOVA followed by Tukey's post hoc tests. Data are represented as the mean ± SEM.

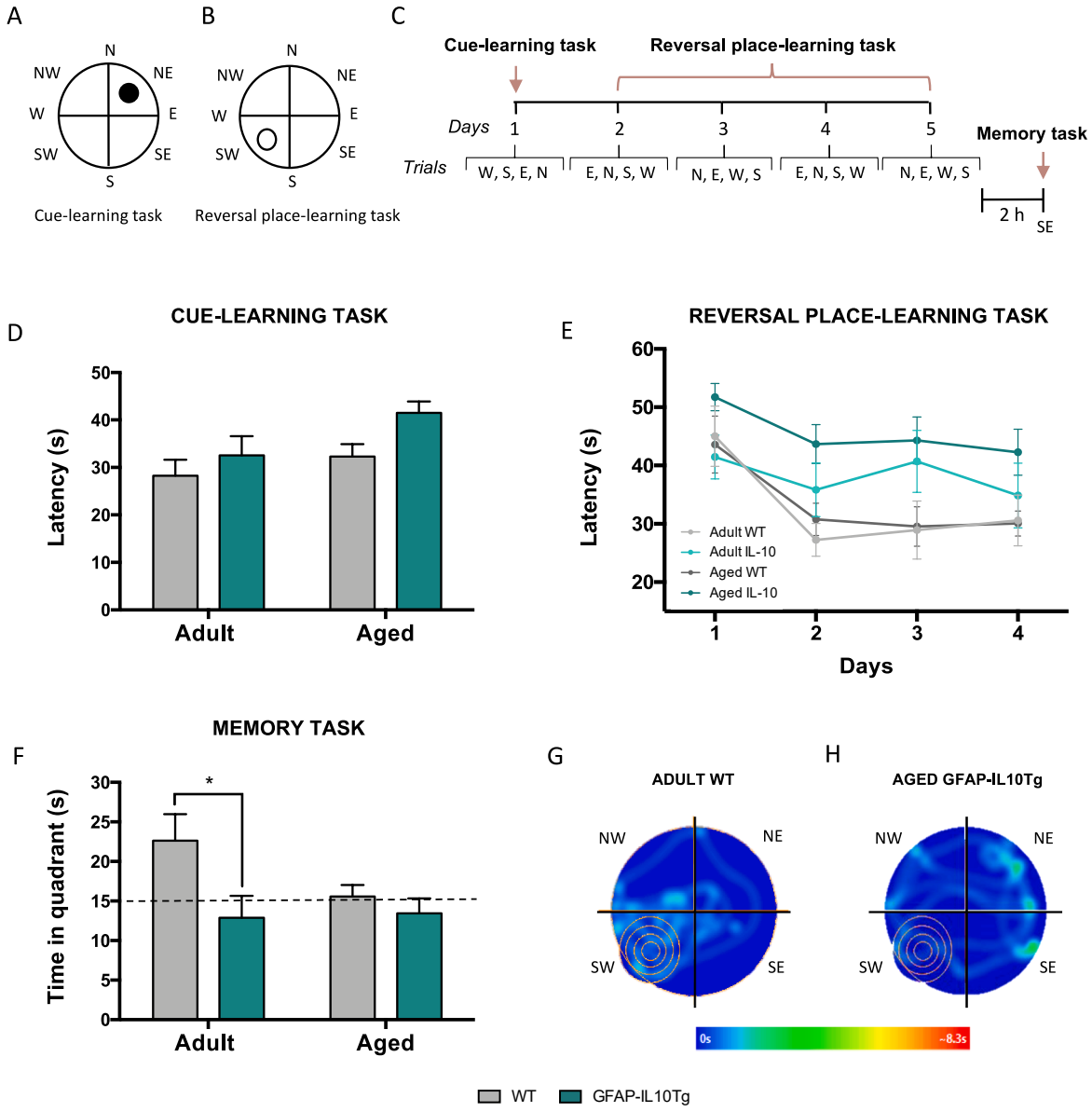

Fig. 4. Short- and long-term spatial learning and memory impairment in GFAP-IL10Tg mice assessed by the visual perceptual (cue) learning and reversal place-learning tasks in the Morris water maze. Swimming-pool representation showing a visible platform (black circle) in the cue-learning task (A) and a hidden platform (white circle) in the place-learning task (B) of the Morris water maze. Temporal scheme of the three paradigms for learning and memory performed in the Morris water maze (C). Graphs show the latency to reach the visible platform on the first day of the test (D) and the hidden platform on the next consecutive four days of the test (E). After platform removal, the time spent in the quadrant where the platform was is represented in the graph (F). Panels showing representative swimming-pool heat-maps indicating mouse path in the memory task (G,H). Statistical analysis was performed by two-way ANOVA followed by Tukey's post hoc tests. *$p < 0.05$. Data are represented as the mean ± SEM. Abbreviations: N; north, NE; northeast, E; east, SE; southeast, S; south, SW; southwest, W; west, NW; northwest.

genotype ($F(1, 32) = 4.65$, $p < 0.05$) on the time required to reach the visible cued platform (Fig. 4D). In the reversal place-learning task for spatial learning and memory, main effects of trial day ($F(3, 122) = 6.90$, $p < 0.001$) and animal group ($F(3, 122) = 8.12$, $p < 0.0001$) were found (Fig. 4E). Here, the aged transgenic mice showed the worst performance in the task, unveiling long-term learning and memory deficits in a reversal task which demands cognitive flexibility (Fig. 4E). Two hours after the last trial, the platform was removed and spatial memory was evaluated measuring the time that animals spent in the quadrant where the platform was previously located (Fig. 4F-H). Our results demonstrated that spatial memory was impaired in GFAP-IL10Tg mice (two-way ANOVA: genotype effect, $F(1, 30) = 6.20$, $p < 0.05$) in adulthood, showing times in the target quadrant similar to that observed in aged WT mice (Fig. 4F). In summary, these paradigms showed that animals with IL-10 overexpression presented hippocampal cognitive deficits in learning acquisition and memory processes.

3.4. Increased IL-10 levels in GFAP-IL10Tg mice without modifications in growth factors or pro-inflammatory cytokines

To address whether the observed neurological and behavioral alterations in transgenic animals correlated with IL-10 overproduction, IL-10 levels in the hippocampus and the serum of animals were measured by the Luminex assay. Our data demonstrated that GFAP-IL10Tg mice presented increased levels of IL-10 in both hippocampal (two-way ANOVA: genotype effect, $F(1, 20) = 21.75$, $p < 0.001$) and serum (two-way ANOVA: genotype effect, $F(1, 13) = 7.63$, $p < 0.05$) samples (Fig. 5A,D). However, no effect of IL-10 expression due to age was

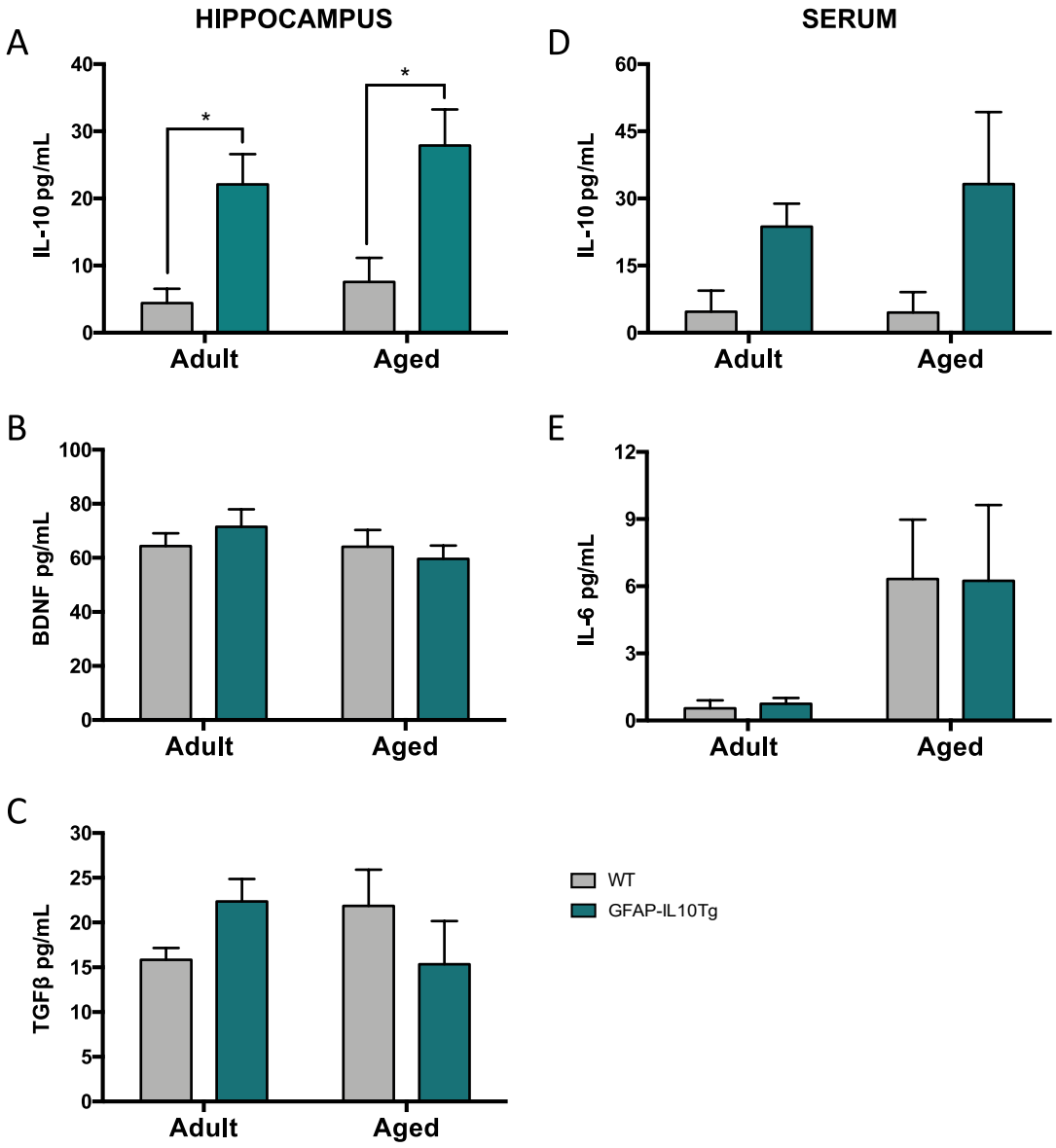

Fig. 5. Increased levels of IL-10 in the hippocampus and the serum of GFAP-IL10Tg mice. Graphs showing quantitative IL-10 (A), BDNF (B) and TGFβ (C) protein expression in the hippocampus, and IL-10 (D) and IL-6 (E) protein expression in the serum of WT and GFAP-IL10Tg mice by Luminex assay. Statistical analysis was performed by two-way ANOVA followed by Tukey's post hoc tests. *$p < 0.05$. Data are represented as the mean ± SEM. Abbreviations: BDNF; brain-derived neurotrophic factor, TGFβ; transforming growth factor-β.

observed for any genotype (Fig. 5A,D).

Because growth factors are involved in the process of neurogenesis, hippocampal BDNF and TGFβ levels were measured. Although a high expression of these factors was detected in all groups studied, no differences by age or genotype were observed (Fig. 5B,C). The levels of pro-inflammatory IL-6, IL-1β and TNF-α cytokines were also measured in the hippocampus and the serum as possible negative regulators of neurogenesis. Very low or undetected levels of these cytokines, without differences among the studied experimental groups, were detected in the hippocampus (data not shown). Only an IL-6 increase in the serum of aged animals (two-way ANOVA: age effect, F (1, 11) = 8.35, $p < 0.05$) was observed regardless the genotype (Fig. 5E).

3.5. Different hippocampal immune cells profile by IL-10 overexpression

Immune cells, especially lymphocytes, macrophages and microglia, play a role in the process of neurogenesis. By flow cytometry, we distinguished three leucocyte populations: non-myeloid cells ($CD11b^-/CD45^+$), high-activated myeloid cells ($CD11b^+/CD45^{high}$) and low-/intermediate-activated myeloid cells ($CD11b^+/CD45^{low/int}$).

$CD11b^-/CD45^+$ cell number increased by age (two-way ANOVA: age effect, F (1, 23) = 16.24, $p < 0.001$), but no differences between WT and GFAP-IL10Tg mice were observed (Fig. 6D). However, the expression of CD45 in these cells was higher in GFAP-IL10Tg respect to WT mice during aging (two-way ANOVA: genotype effect, F (1, 25) = 16.95, $p < 0.001$) (Fig. 6E). On the other hand, no effect by age was observed in the number of $CD11b^+/CD45^+$ cells (Fig. 6F,I). However, two-way ANOVA revealed a main effect of the genotype on the cell number of $CD11b^+/CD45^{high}$ (F (1, 25) = 24.68, $p < 0.0001$) (Fig. 6F) and $CD11b^+/CD45^{low/int}$ (F (1, 13) = 8.44, $p < 0.05$) (Fig. 6I). Our results showed that CD45 expression on $CD11b^+/CD45^{high}$ cells decreases in WT mice with aging, whereas GFAP-IL10Tg mice already present similar CD45 levels to those observed in aged WT mice since adulthood (two-way ANOVA: age effect, F (1, 24) = 11.78, $p < 0.01$; genotype effect, F (1, 24) = 15.60, $p < 0.001$; interaction effect, F (1, 24) = 6.98, $p < 0.05$) (Fig. 6G). In contrast, CD45 expression on $CD11b^+/CD45^{low/int}$ cells was increased

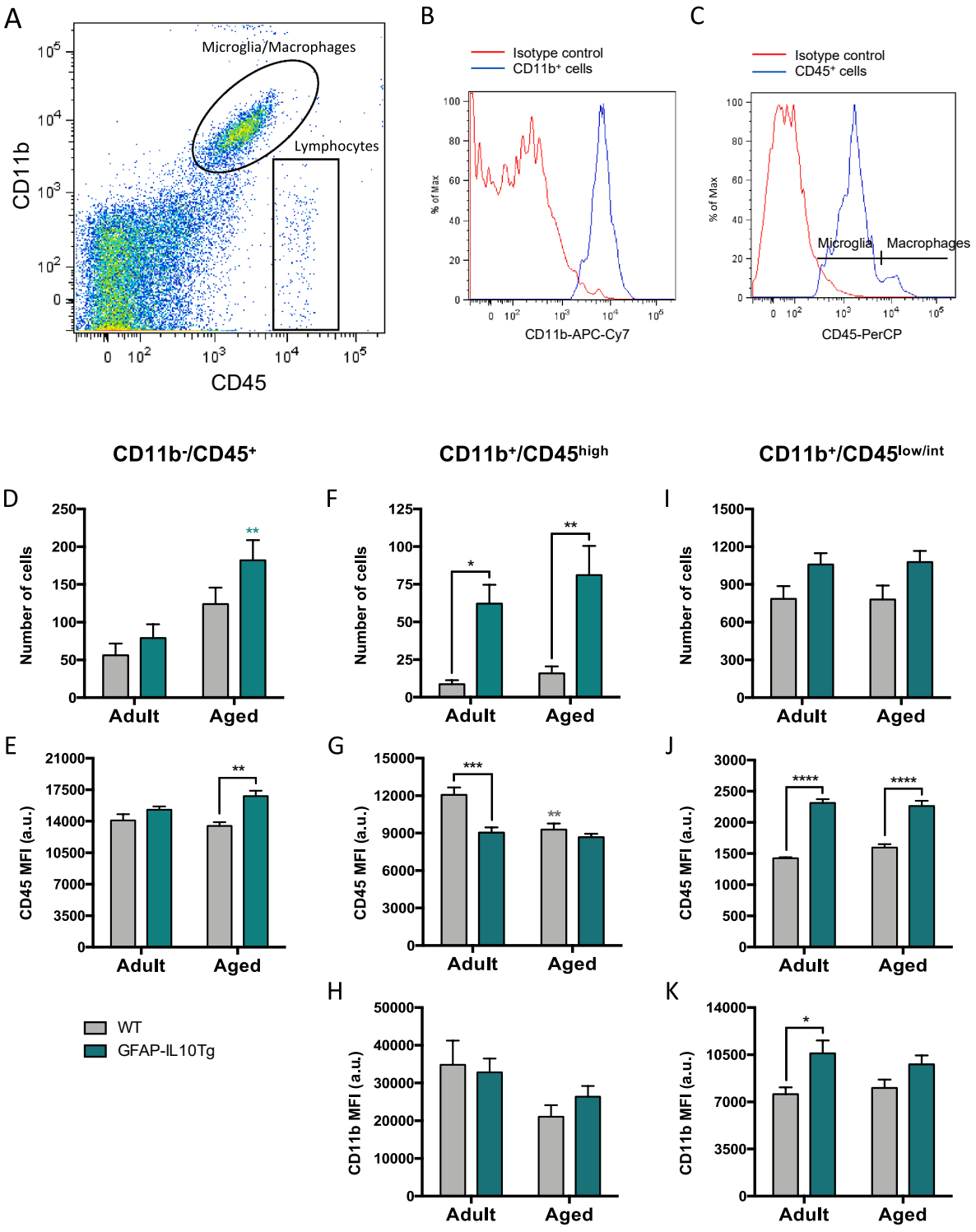

Fig. 6. Elevated number of CD11b^{+}/CD45^{high} cells and high activation of CD11b^{+}/CD45$^{low/int}$ cells in GFAP-IL10Tg mice. Gate strategy showing the selection region of myeloid (CD11b^{+}/CD45^{+}) and non-myeloid (CD11b^{-}/CD45^{+}) cell populations by CD11b and CD45 expression (A). Histograms representing isotype control and positive staining of CD11b-APC-Cy7 (B) and CD45-PerCP (C) isotypes/antibodies. Histogram (C) is showing the separation between CD11b^{+}/CD45$^{low/int}$ (microglia) and CD11b^{+}/CD45^{high} (macrophages) populations by CD45-PerCP fluorescence intensity. Graphs showing the number of CD11b^{-}/CD45^{+} (D), CD11b^{+}/CD45^{high} (F) and CD11b^{+}/CD45$^{low/int}$ (I) cells in the hippocampus of WT and GFAP-IL10Tg mice. CD45 (E, G, J) and CD11b (H, K) cell expression is represented by the mean fluorescent intensity in CD11b^{-}/CD45^{+} (E), CD11b^{+}/CD45^{high} (G, H) and CD11b^{+}/CD45$^{low/int}$ (J, K) cells. Statistical analysis was performed by two-way ANOVA followed by Tukey's post hoc tests. Grey and cyan asterisks refer to significant differences by age in WT and GFAP-IL10Tg mice, respectively. *$p < 0.05$, **$p < 0.01$, ***$p < 0.001$. Data are represented as the mean ± SEM. Abbreviations: MFI; mean fluorescence intensity, a.u.; arbitrary units. (For interpretation of the references to colour in this figure legend, the reader is referred to the web version of this article.)

by IL-10 overexpression at both ages (two-way ANOVA: genotype effect, $F(1, 26) = 189.00$, $p < 0.0001$) (Fig. 6J). Regarding CD11b expression, two-way ANOVA showed a main effect of age ($F(1, 24) = 6.25$, $p < 0.05$) in CD11b^{+}/CD45^{high} cells (Fig. 6H) and a main effect of genotype ($F(1, 26) = 10.98$, $p < 0.01$) in CD11b^{+}/CD45$^{low/int}$ cells (Fig. 6K). Post-hoc analysis revealed a higher CD11b level in the CD11b^{+}/CD45$^{low/int}$ cells from adult GFAP-IL10Tg mice with respect to WT animals (Fig. 6K).

3.6. Altered microglia-neuron communication in GFAP-IL10Tg mice

Considering that microglia/macrophage (CD11b^{+}/CD45^{+}) populations were different between WT and GFAP-IL10Tg mice during adulthood, we studied myeloid receptors that are involved in neuronal communication as possible modulators of the neurogenesis impairment observed in transgenic mice. CD200R, SIRPα and CX3CR1 expression

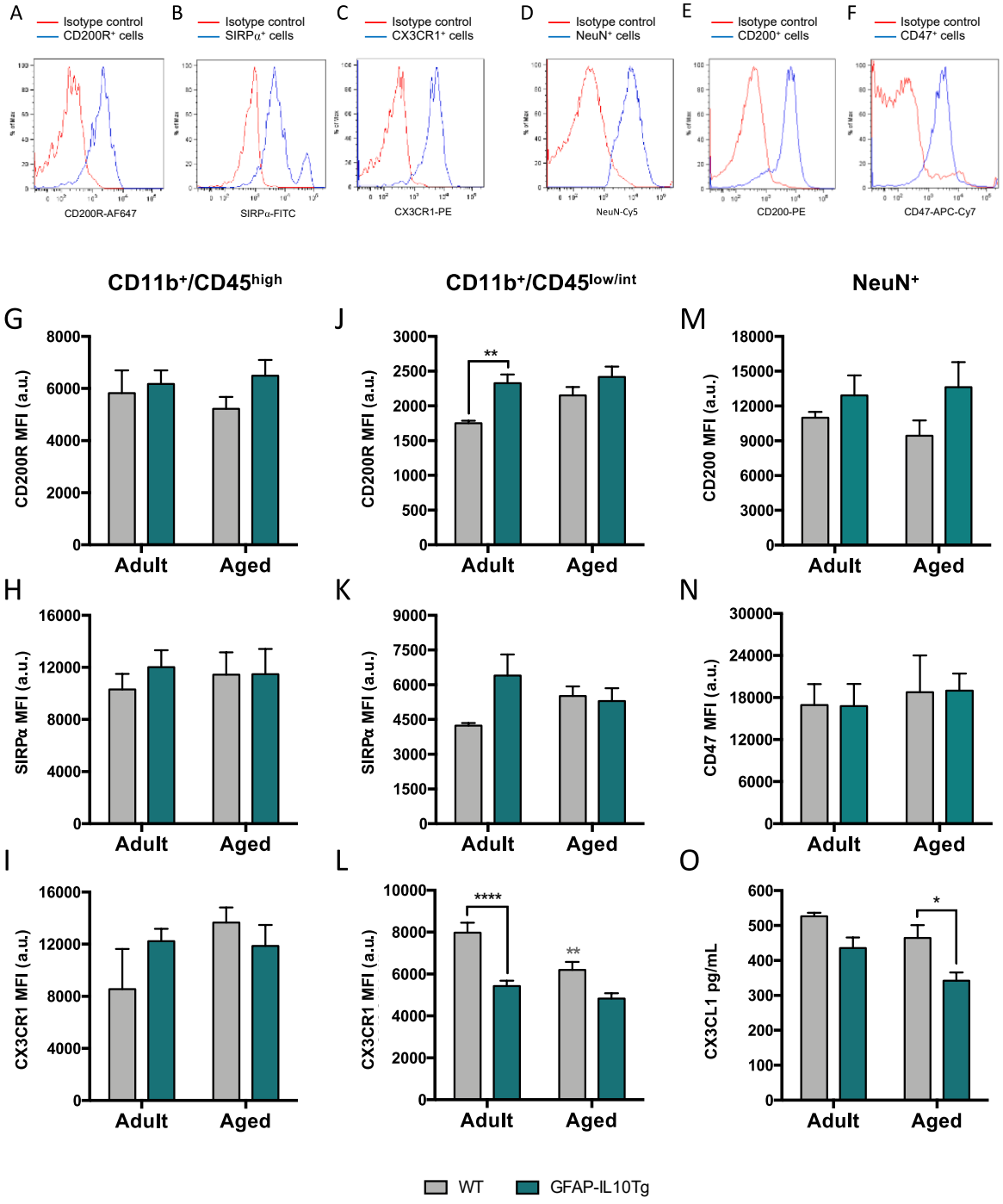

Fig. 7. Altered homeostatic receptors in CD11b^{+}/CD45$^{low/int}$ cells of GFAP-IL10Tg mice. Histograms representing isotype control and positive staining of CD200R-AlexaFluor-647 (A), SIRPα-FITC (B), CX3CR1-PE (C), NeuN-Cy5 (D), CD200-PE (E), CD47-APC-Cy7 (F) isotypes/antibodies. Cell expression of CD200R (G, J), SIRPα (H, K) and CX3CR1 (I, L) is represented by the mean fluorescence intensity in CD11b^{+}/CD45^{high} (G-I) and CD11b^{+}/CD45$^{low/int}$ (J-L) hippocampal cells. CD200 (M) and CD47 (N) cell expression is represented by the mean fluorescence intensity in hippocampal NeuN^{+} cells, whereas CX3CL1 (O) expression is shown by Luminex assay in hippocampal lysates. Statistical analysis was performed by two-way ANOVA followed by Tukey's post hoc tests. Grey asterisks refer to significant differences by age in WT mice. *$p < 0.05$, **$p < 0.01$, ****$p < 0.0001$. Data are represented as the mean ± SEM. Abbreviations: MFI; mean fluorescence intensity, a.u.; arbitrary units.

was analyzed separately in $CD11b^+/CD45^{high}$ and $CD11b^+/CD45^{low/int}$ cells. No differences of CD200R, SIRPα or CX3CR1 expression due to the effect of age or genotype were observed in $CD11b^+/CD45^{high}$ cells (Fig. 7G-I). However, in $CD11b^+/CD45^{low/int}$ cells, both age and genotype modified the expression of CD200R (two-way ANOVA: age effect, $F(1, 25) = 4.41$, $p < 0.05$; genotype effect, $F(1, 25) = 12.87$, $p < 0.01$) and CX3CR1 (two-way ANOVA: age effect, $F(1, 26) = 11.28$, $p < 0.01$; genotype effect, $F(1, 26) = 30.51$, $p < 0.0001$) (Fig. 7J,L). A tendency, albeit not statistically significant, for SIRPα levels to increase by age and genotype was observed (Fig. 7K). Our results showed that CD200R levels were increased under IL-10 transgenic overproduction reaching levels similar to that observed during normal aging (Fig. 7J). On the contrary, CX3CR1 expression was decreased in adult transgenic mice and in aged WT mice (Fig. 7L).

Regarding neurons, our data showed a similar number of $NeuN^+$ cells in all groups studied (data not shown). Expression of CD200, CD47 and CX3CL1, the neuronal ligands of CD200R, SIRPα and CX3CR1, respectively, was also studied. No significant differences in CD200 or CD47 expression by age or genotype were detected in the neuronal population (Fig. 7M,N). However, an age- and genotype-dependent reduction of total CX3CL1 levels was observed (two-way ANOVA: age effect, $F(1, 20) = 8.17$, $p < 0.01$; genotype effect, $F(1, 20) = 15.49$, $p < 0.001$) (Fig. 7O). Post-hoc analysis revealed that animals with IL-10 overproduction presented lower CX3CL1 levels than did WT animals specifically during aging (Fig. 7O).

4. Discussion

The present study shows that chronic transgenic IL-10 overproduction in the CNS induces a hippocampal microglial phenotype in adult mice very similar to that observed in the physiological aging, which could be anticipating the age-related decreased neurogenesis and cognitive deficits. To the best of our knowledge, this work is the first to show a negative effect of chronic IL-10 overproduction on hippocampal neurogenesis of the adult and the aged brain under physiological conditions *in vivo*.

During aging, the brain microenvironment has been reported to be modified to a pro-inflammatory status characterized by high oxidative stress, pro-inflammatory cytokines, and microglial activation (Nakanishi and Wu, 2009; Sierra et al., 2007; Udeochu et al., 2016). Specifically, the hippocampus is one of the most affected brain areas by age (Barrientos et al., 2015; Mattson and Magnus, 2006; Ojo et al., 2015). In this area, neurogenesis decreases dramatically with normal aging, impacting cognitive functions (Drapeau et al., 2003; Klempin and Kempermann, 2007; Villeda et al., 2011). Since neurogenic niches are intimately associated with the microenvironment, and it is known that inflammation is detrimental to the process of neurogenesis, it is plausible to think that the neuroinflammation of the aged brain is a critical factor for the decrease in the generation of new neurons during aging. In this context, we analyzed adult and aged hippocampal neurogenesis in transgenic animals with an anti-inflammatory microenvironment generated by the astrocyte-targeted overproduction of IL-10.

Our observations showing both fewer DCX^+ and $BrdU^+$ cells in aged animals are consistent with the lower hippocampal neurogenesis reported during aging (Klempin and Kempermann, 2007; Kuhn et al., 1996; Kuipers et al., 2015). Moreover, in these animals, we also reported spatial memory impairment as a principal feature of hippocampal affectation. Surprisingly, our results demonstrated that transgenic animals with overexpression of the anti-inflammatory IL-10 cytokine present lower hippocampal neurogenesis than do WT mice during adulthood. In concordance with the decrease of new neuron formation, IL-10 overproduction impaired hippocampal-dependent spatial learning and memory, as was determined by the T-maze and the Morris water maze. These tests allowed to screen the effects on cognitive function under different anxiety-levels and cognitive demands in terms of temporal requirements, visual perceptual learning and cognitive flexibility, which have been previously described to be sensitive to reduction of neurogenesis (Anacker and Hen, 2017; Forte et al., 2021) and also allow to define behavioral signatures depending on genotype and aging (Giménez-Llort et al., 2021). These cognitive deficits also corroborated the lower excitability of hippocampal synapses and the absence of long-term potentiation previously described in adult GFAP-IL10Tg animals (Almolda et al., 2015). In line with our observations, it has been reported that adeno-associated virus-mediated IL-10 expression exacerbates hippocampal-dependent memory impairment (Chakrabarty et al., 2015), whereas IL-10 deficiency partially restores this cognitive deficit (Guillot-Sestier et al., 2015) in Alzheimer's disease transgenic mouse models.

The negative effect of chronic IL-10 overexpression on hippocampal neurogenesis reported here is consistent with a previous study reporting that IL-10 administration decreases the number of DCX^+ cells in the SVZ, while in IL-10-KO mice DCX expression is increased (Perez-Asensio et al., 2013). On the contrary, another study reported that IL-10 gene delivery by adeno-associated viruses enhances hippocampal neurogenesis and improves cognitive function in an Alzheimer's murine model (Kiyota et al., 2012). As a possible cause of the different IL-10 effects, in the Kiyota et al. (2012) study, IL-10 was administered only at one time point, while in our work a chronic astrocyte-dependent IL-10 production exists since birth. Moreover, unlike our study, neurogenesis was enhanced by IL-10 injections in a pathological situation. To study modifications in neuronal precursor proliferation as a possible explanation of the reduced neurogenesis in GFAP-IL10Tg mice, the number of cells incorporating the BrdU synthetic nucleotide was quantified before the apoptosis period. At this time, no differences in the number of proliferating $BrdU^+$ cells were detected by IL-10 overexpression. Interestingly, our data showing a significant reduction in the number of $BrdU^+$ cells after the apoptosis period in transgenic mice with respect to WT mice, demonstrate that IL-10 overexpression negatively affects the survival of hippocampal NSCs, leading to a decreased neurogenesis during adulthood. However, no differences in either the expression of hippocampal BDNF or TGFβ, which promote neural survival/differentiation (Goldman et al., 1997; Lee et al., 2002; Taliaz et al., 2010), were detected between WT and GFAP-IL10Tg mice. These data rule out the involvement of these factors in the decreased NSC survival produced by IL-10 overexpression.

Our results showing greater IL-10 levels in the hippocampus and serum of transgenic mice when compared to WT, point to IL-10 as a key regulator of hippocampal neurogenesis. IL-10 intraventricular administration has been shown to maintain NSCs in an undifferentiated transition state by a direct effect of this cytokine on the NSCs allocated in the SVZ niche (Pereira et al., 2015; Perez-Asensio et al., 2013). However, as previously reported by Perez-Asensio and collaborators (2013), our work demonstrates that neither WT nor GFAP-IL10Tg animals express IL-10 receptor in NSCs of the hippocampal SGZ niche, and therefore, IL-10 must be indirectly acting on neurogenesis regulation. In this way, immune cells, and especially microglial cells, are highly dependent upon environmental signals (Bennett et al., 2018; Gosselin et al., 2014; Lavin et al., 2014) and play an important role in the process of neurogenesis (Carpentier and Palmer, 2009; Kokaia et al., 2012; Ziv and Schwartz, 2008). Here, we observed that transgenic animals present microglial modifications in markers of general activation (CD45 and CD11b) and markers involved in neuronal communication (CD200R and CX3CR1). Curiously, the specific microglial phenotype acquired by IL-10 overexpression in both age groups was very similar to that observed in normal aging. This similar phenotype between adult GFAP-IL10Tg and aged WT microglia had already been found in our previous study, where we showed an increased microglial cell density, high IBA1 expression and upregulation of phagocytic markers in GFAP-IL10Tg mice (Sanchez-Molina et al., 2021).

In concordance with our results, microglial pro-inflammatory activation has been reported specifically to affect hippocampal survival of newborn cells rather than cell proliferation or differentiation (Bastos

et al., 2008; Ekdahl et al., 2003). Specifically, the present work shows CD200R increase and CX3CR1 decrease in transgenic mice and during physiological aging. Generally, CD200R-CD200 (Manich et al., 2019) and CX3CR1-CX3CL1 (Cardona et al., 2006) interactions maintain microglia in a homeostatic state characterized by anti-inflammatory signaling pathways (Biber et al., 2007; Hu et al., 2014; Linnartz and Neumann, 2013). Disruption of these interactions upon aging and its association with age-related microglial activation has been previously described (Jurgens and Johnson, 2012). Specifically, decreased levels of CD200 (Cox et al., 2012; Frank et al., 2006; Lyons et al., 2007) and CX3CL1 (Bachstetter et al., 2011; Lyons et al., 2009; Vukovic et al., 2012; Wynne et al., 2010) neuronal ligands have been reported in aged rodents. However, to the best of our knowledge, our findings demonstrate for the first time different protein expression of CD200R and CX3CR1 microglial receptors with normal aging. Interestingly, research developed in the last decade has demonstrated that microglia-neuron communication is involved in hippocampal neurogenesis. As an example, administration of the neuronal ligand CD200 restores neurogenesis in a mouse model of Alzheimer's disease coinciding with an anti-inflammatory microglial status. Nevertheless, CD200 overexpression did not enhance neurogenesis in WT mice (Varnum et al., 2015). Considering these data, the higher CD200R expression that we have reported in aged and transgenic animals could be trying to compensate for the lower neurogenesis observed in these animals. On the other hand, disruption of CX3CR1-CX3CL1 dialogue negatively regulates hippocampal neurogenesis by increased production of IL-1β, leading to a pro-inflammatory scenario (Bachstetter et al., 2011). Thus, our findings showing a decrease of CX3CR1 and CX3CL1 expression in GFAP-IL10Tg mice are in concordance with previous studies reporting their correlation with neurogenesis decline (Bachstetter et al., 2011; Reshef et al., 2017; Vukovic et al., 2012). In general, alterations of "do-not-eat-me" signaling result in a pro-inflammatory microenvironment shift affecting the production of new neurons. Here, we identify that homeostatic microglial receptors are altered by both IL-10 overexpression and normal aging. However, the levels of the main pro-inflammatory cytokines negatively involved in the process of neurogenesis, such as IL-6, IL-1β and TNF-α, were very low without differences between WT and GFAP-IL10Tg mice. Likewise, no differences in BDNF and TGFβ expression were detected by aging or IL-10 overproduction. An important consideration is the fact that microglial receptors, neuronal ligands and cytokines were measured in the whole hippocampus, and therefore, possible changes of these molecules in the dentate gyrus could be diluted by the remaining hippocampal structures.

Taken together, our results suggest that the IL-10 effect on neurogenesis could be mediated by a disruption in the normal cell-to-cell contact between microglia and neurons through the effects of IL-10 on neurons, one of the principal cells expressing the IL-10R in the dentate gyrus of transgenic animals (Recasens et al., 2019). In this line, Kiyota and colleagues (2012) demonstrated that microglia pretreated with IL-10 enhance NSCs proliferation and survival in direct co-cultures. Nonetheless, a microglial-conditioned medium through indirect (transwell) co-cultures with IL-10-treated microglia had no effects on the neural population (Kiyota et al., 2012). These findings support the need for direct microglia-neuron contact for a correct neurogenesis promotion.

Although IL-10 has usually been described as an anti-inflammatory cytokine with neuroprotective functions (Burmeister and Marriott, 2018; Lobo-Silva et al., 2016), its temporal expression is critical for its effect. Moreover, the IL-10 effect has recently been described as dual, including anti- and pro-inflammatory properties depending on the binding affinity for the IL-10 receptor and its intracellular signaling (Saxton et al., 2021). Thus, here we report a microglial shift toward a more activated phenotype similar to that of aged microglia, with a detrimental effect on hippocampal neurogenesis in animals chronically overexpressing IL-10 since postnatal development.

5. Conclusions

This work shows the importance of the microenvironment on microglial cells and their relationship with neurogenesis. Interestingly, we have demonstrated that chronic anti-inflammatory IL-10 overproduction has a similar effect to physiological aging on the hippocampus. Specifically, in transgenic animals and WT with normal aging, hippocampal neurogenesis and memory are impaired together with alterations in the microglia-neuron communication. Likely, IL-10 overexpression modifies microglial receptors involved in neuronal communication, resulting in reduced neurogenesis. This study emphasizes the variety of possibilities that a specific cytokine can exert depending on the moment and the time in which it is expressed. Thus, we describe new properties of IL-10 in hippocampal neurogenesis *in vivo*.

Declaration of Competing Interest

The authors declare that they have no known competing financial interests or personal relationships that could have appeared to influence the work reported in this paper.

Acknowledgments

The authors wish to thank Dr. Manuela Costa for helping with the flow cytometer and to Mr. Chuck Simmons, a native English-speaking instructor of English, for the proofreading of this manuscript. The graphical abstract was created with BioRender.com.

Funding

This work was supported by the Spanish Ministry of Economy and Business (BFU2014-55459 and BFU2017-87843-R).

References

Aharoni, R., Arnon, R., Eilam, R., 2005. Neurogenesis and neuroprotection induced by peripheral immunomodulatory treatment of experimental autoimmune encephalomyelitis. J. Neurosci. 25 (36), 8217–8228. https://doi.org/10.1523/JNEUROSCI.1859-05.2005.

Akkermann, R., Beyer, F., Küry, P., 2017. Heterogeneous populations of neural stem cells contribute to myelin repair. Neural Regen. Res. 12 (4), 509–517. https://doi.org/10.4103/1673-5374.204999.

Almolda, B., de Labra, C., Barrera, I., Gruart, A., Delgado-Garcia, J.M., Villacampa, N., Vilella, A., Hofer, M.J., Hidalgo, J., Campbell, I.L., González, B., Castellano, B., 2015. Alterations in microglial phenotype and hippocampal neuronal function in transgenic mice with astrocyte-targeted production of interleukin-10. Brain Behav. Immun. 45, 80–97. https://doi.org/10.1016/j.bbi.2014.10.015.

Altman, J., Das, G.D., 1965. Autoradiographic and histological evidence of postnatal hippocampal neurogenesis in rats. J. Comp. Neurol. 124 (3), 319–335. https://doi.org/10.1002/cne.901240303.

Anacker, C., Hen, R., 2017. Adult hippocampal neurogenesis and cognitive flexibility – linking memory and mood. Nat. Rev. Neurosci. 18 (6), 335–346. https://doi.org/10.1038/nrn.2017.45.

Bachstetter, A.D., Morganti, J.M., Jernberg, J., Schlunk, A., Mitchell, S.H., Brewster, K. W., Hudson, C.E., Cole, M.J., Harrison, J.K., Bickford, P.C., Gemma, C., 2011. Fractalkine and CX 3 CR1 regulate hippocampal neurogenesis in adult and aged rats. Neurobiol. Aging 32 (11), 2030–2044. https://doi.org/10.1016/j.neurobiolaging.2009.11.022.

Barrientos, R.M., Kitt, M.M., Watkins, L.R., Maier, S.F., 2015. Neuroinflammation in the normal aging hippocampus. Neuroscience 309, 84–99. https://doi.org/10.1016/j.neuroscience.2015.03.007.

Bastos, G.N., Moriya, T., Inui, F., Katura, T., Nakahata, N., 2008. Involvement of cyclooxygenase-2 in lipopolysaccharide-induced impairment of the newborn cell survival in the adult mouse dentate gyrus. Neuroscience 155 (2), 454–462. https://doi.org/10.1016/j.neuroscience.2008.06.020.

Battista, D., Ferrari, C.C., Gage, F.H., Pitossi, F.J., 2006. Neurogenic niche modulation by activated microglia: transforming growth factor beta increases neurogenesis in the adult dentate gyrus. Eur. J. Neurosci. 23 (1), 83–93. https://doi.org/10.1111/j.1460-9568.2005.04539.x.

Bennett, F.C., Bennett, M.L., Yaqoob, F., Mulinyawe, S.B., Grant, G.A., Hayden Gephart, M., Plowey, E.D., Barres, B.A., 2018. A combination of ontogeny and CNS environment establishes microglial identity. Neuron 98 (6), 1170–1183.e8. https://doi.org/10.1016/j.neuron.2018.05.014.

Biber, K., Neumann, H., Inoue, K., Boddeke, H.W., 2007. Neuronal 'On' and 'Off' signals control microglia. Trends Neurosci. 30 (11), 596–602. https://doi.org/10.1016/j.tins.2007.08.007.

Bond, A.M., Berg, D.A., Lee, S., Garcia-Epelboim, A.S., Adusumilli, V.S., Ming, G.L., Song, H., 2020. Differential timing and coordination of neurogenesis and astrogenesis in developing mouse hippocampal subregions. Brain Sci. 10 (12), 909. https://doi.org/10.3390/brainsci10120909.

Bondolfi, L., Ermini, F., Long, J.M., Ingram, D.K., Jucker, M., 2004. Impact of age and caloric restriction on neurogenesis in the dentate gyrus of C57BL/6 mice. Neurobiol. Aging 25 (3), 333–340. https://doi.org/10.1016/S0197-4580(03)00083-6.

Borsini, A., Zunszain, P.A., Thuret, S., Pariante, C.M., 2015. The role of inflammatory cytokines as key modulators of neurogenesis. Trends Neurosci. 38 (3), 145–157. https://doi.org/10.1016/j.tins.2014.12.006.

Burmeister, A.R., Marriott, I., 2018. The interleukin-10 family of cytokines and their role in the CNS. Front. Cell. Neurosci. 12, 458.

Butovsky, O., Ziv, Y., Schwartz, A., Landa, G., Talpalar, A.E., Pluchino, S., Martino, G., Schwartz, M., 2006. Microglia activated by IL-4 or IFN-gamma differentially induce neurogenesis and oligodendrogenesis from adult stem/progenitor cells. Mol. Cell. Neurosci. 31 (1), 149–160. https://doi.org/10.1016/j.mcn.2005.10.006.

Cacci, E., Claasen, J.H., Kokaia, Z., 2005. Microglia-derived tumor necrosis factor-alpha exaggerates death of newborn hippocampal progenitor cells in vitro. J. Neurosci. Res. 80 (6), 789–797. https://doi.org/10.1002/jnr.20531.

Cardona, A.E., Pioro, E.P., Sasse, M.E., Kostenko, V., Cardona, S.M., Dijkstra, I.M., Huang, D., Kidd, G., Dombrowski, S., Dutta, R., Lee, J.C., Cook, D.N., Jung, S., Lira, S.A., Littman, D.R., Ransohoff, R.M., 2006. Control of microglial neurotoxicity by the fractalkine receptor. Nat. Neurosci. 9 (7), 917–924. https://doi.org/10.1038/nn1715.

Carpentier, P.A., Palmer, T.D., 2009. Immune influence on adult neural stem cell regulation and function. Neuron 64 (1), 79–92. https://doi.org/10.1016/j.neuron.2009.08.038.

Chakrabarty, P., Li, A., Ceballos-Diaz, C., Eddy, J.A., Funk, C.C., Moore, B., DiNunno, N., Rosario, A.M., Cruz, P.E., Verbeeck, C., Sacino, A., Nix, S., Janus, C., Price, N.D., Das, P., Golde, T.E., 2015. IL-10 alters immunoproteostasis in APP mice, increasing plaque burden and worsening cognitive behavior. Neuron 85 (3), 519–533. https://doi.org/10.1016/j.neuron.2014.11.020.

Cornejo, F., von Bernhardi, R., 2016. Age-Dependent Changes in the Activation and Regulation of Microglia. Adv. Exp. Med. Biol. 949, 205–226. https://doi.org/10.1007/978-3-319-40764-7_10.

Cox, F.F., Carney, D., Miller, A.M., Lynch, M.A., 2012. CD200 fusion protein decreases microglial activation in the hippocampus of aged rats. Brain Behav. Immun. 26 (5), 789–796. https://doi.org/10.1016/j.bbi.2011.10.004.

Deng, W., Aimone, J.B., Gage, F.H., 2010. New neurons and new memories: how does adult hippocampal neurogenesis affect learning and memory? Nat. Rev. Neurosci. 11 (5), 339–350. https://doi.org/10.1038/nrn2822.

Drapeau, E., Mayo, W., Aurousseau, C., Le Moal, M., Piazza, P.V., Abrous, D.N., 2003. Spatial memory performances of aged rats in the water maze predict levels of hippocampal neurogenesis. Proc. Natl. Acad. Sci. U.S.A. 100 (24), 14385–14390. https://doi.org/10.1073/pnas.2334169100.

Dupret, D., Revest, J.-M., Koehl, M., Ichas, F., De Giorgi, F., Costet, P., Abrous, D.N., Piazza, P.V., Mayeux, R., 2008. Spatial relational memory requires hippocampal adult neurogenesis. PLoS ONE 3 (4), e1959. https://doi.org/10.1371/journal.pone.0001959.

Ekdahl, C.T., Claasen, J.H., Bonde, S., Kokaia, Z., Lindvall, O., 2003. Inflammation is detrimental for neurogenesis in adult brain. Proc. Natl. Acad. Sci. U.S.A. 100 (23), 13632–13637. https://doi.org/10.1073/pnas.2234031100.

Encinas, J.M., Michurina, T.V., Peunova, N., Park, J.H., Tordo, J., Peterson, D.A., Fishell, G., Koulakov, A., Enikolopov, G., 2011. Division-coupled astrocytic differentiation and age-related depletion of neural stem cells in the adult hippocampus. Cell Stem Cell 8 (5), 566–579. https://doi.org/10.1016/j.stem.2011.03.010.

Eriksson, P.S., Perfilieva, E., Björk-Eriksson, T., Alborn, A.M., Nordborg, C., Peterson, D.A., Gage, F.H., 1998. Neurogenesis in the adult human hippocampus. Nat. Med. 4 (11), 1313–1317. https://doi.org/10.1038/3305.

Forte, N., Boccella, S., Tunisi, L., Fernández-Rilo, A.C., Imperatore, R., Iannotti, F.A., De Risi, M., Iannotta, M., Piscitelli, F., Capasso, R., De Girolamo, P., De Leonibus, E., Maione, S., Di Marzo, V., Cristino, L., 2021. Orexin-A and endocannabinoids are involved in obesity-associated alteration of hippocampal neurogenesis, plasticity, and episodic memory in mice. Nat. Commun. 12 (1), 6137. https://doi.org/10.1038/s41467-021-26388-4.

Frank, M.G., Barrientos, R.M., Biedenkapp, J.C., Rudy, J.W., Watkins, L.R., Maier, S.F., 2006. mRNA up-regulation of MHC II and pivotal pro-inflammatory genes in normal brain aging. Neurobiol. Aging 27 (5), 717–722. https://doi.org/10.1016/j.neurobiolaging.2005.03.013.

Garthe, A., Behr, J., Kempermann, G., Earley, R.L., 2009. Adult-generated hippocampal neurons allow the flexible use of spatially precise learning strategies. PLoS ONE 4 (5), e5464. https://doi.org/10.1371/journal.pone.0005464.

Giménez-Llort, L., García, Y., Buccieri, K., Revilla, S., Suñol, C., Cristofol, R., Sanfeliu, C., 2010. Gender-Specific neuroimmunoendocrine response to treadmill exercise in 3xTg-AD mice. Int. J. Alzheimers Dis. 2010, 1–17. https://doi.org/10.4061/2010/128354.

Giménez-Llort, L., Marin-Pardo, D., Marazuela, P., Hernández-Guillamón, M., 2021. Survival bias and crosstalk between chronological and behavioral age: age- and genotype-sensitivity tests define behavioral signatures in middle-aged, old, and long-lived mice with normal and AD-associated aging. Biomedicines. 9 (6), 636. https://doi.org/10.3390/biomedicines9060636.

Goldman, S.A., Kirschenbaum, B., Harrison-Restelli, C., Thaler, H.T., 1997. Neuronal precursors of the adult rat subependymal zone persist into senescence, with no decline in spatial extent or response to BDNF. J. Neurobiol. 32 (6), 554–566. https://doi.org/10.1002/(sici)1097-4695(19970605)32:6<554::aid-neu2>3.0.co;2-z.

Goshen, I., Kreisel, T., Ben-Menachem-Zidon, O., Licht, T., Weidenfeld, J., Ben-Hur, T., Yirmiya, R., 2008. Brain interleukin-1 mediates chronic stress-induced depression in mice via adrenocortical activation and hippocampal neurogenesis suppression. Mol. Psychiatry 13 (7), 717–728. https://doi.org/10.1038/sj.mp.4002055.

Gosselin, D., Link, V.M., Romanoski, C.E., Fonseca, G.J., Eichenfield, D.Z., Spann, N.J., Stender, J.D., Chun, H.B., Garner, H., Geissmann, F., Glass, C.K., 2014. Environment drives selection and function of enhancers controlling tissue-specific macrophage identities. Cell 159 (6), 1327–1340. https://doi.org/10.1016/j.cell.2014.11.023.

Guillot-Sestier, M.V., Doty, K.R., Gate, D., Rodriguez Jr, J., Leung, B.P., Rezai-Zadeh, K., Town, T., 2015. Il10 deficiency rebalances innate immunity to mitigate Alzheimer-like pathology. Neuron 85 (3), 534–548. https://doi.org/10.1016/j.neuron.2014.12.068.

Hirabayashi, Y., Gotoh, Y., 2005. Stage-dependent fate determination of neural precursor cells in mouse forebrain. Neurosci. Res. 51 (4), 331–336. https://doi.org/10.1016/j.neures.2005.01.004.

Hu, X., Liou, A.K., Leak, R.K., Xu, M., An, C., Suenaga, J., Shi, Y., Gao, Y., Zheng, P., Chen, J., 2014. Neurobiology of microglial action in CNS injuries: receptor-mediated signaling mechanisms and functional roles. Prog. Neurobiol. 119–120, 60–84. https://doi.org/10.1016/j.pneurobio.2014.06.002.

Hueston, C.M., O'Leary, J.D., Hoban, A.E., Kozareva, D.A., Pawley, L.C., O'Leary, O.F., Cryan, J.F., Nolan, Y.M., 2018. Chronic interleukin-1β in the dorsal hippocampus impairs behavioural pattern separation. Brain Behav. Immun. 74, 252–264. https://doi.org/10.1016/j.bbi.2018.09.015.

Imayoshi, I., Sakamoto, M., Ohtsuka, T., Kageyama, R., 2009. Continuous neurogenesis in the adult brain. Dev. Growth Differ. 51 (3), 379–386. https://doi.org/10.1111/j.1440-169X.2009.01094.x.

Jurgens, H.A., Johnson, R.W., 2012. Dysregulated neuronal-microglial cross-talk during aging, stress and inflammation. Exp. Neurol. 233 (1), 40–48. https://doi.org/10.1016/j.expneurol.2010.11.014.

Kaplan, M.S., Hinds, J.W., 1977. Neurogenesis in the adult rat: electron microscopic analysis of light radioautographs. Science 197 (4308), 1092–1094. https://doi.org/10.1126/science.887941.

Kee, N., Teixeira, C.M., Wang, A.H., Frankland, P.W., 2007. Preferential incorporation of adult-generated granule cells into spatial memory networks in the dentate gyrus. Nat. Neurosci. 10 (3), 355–362. https://doi.org/10.1038/nn1847.

Kiyota, T., Ingraham, K.L., Swan, R.J., Jacobsen, M.T., Andrews, S.J., Ikezu, T., 2012. AAV serotype 2/1-mediated gene delivery of anti-inflammatory interleukin-10 enhances neurogenesis and cognitive function in APP+PS1 mice. Gene Ther. 19 (7), 724–733. https://doi.org/10.1038/gt.2011.126.

Kiyota, T., Okuyama, S., Swan, R.J., Jacobsen, M.T., Gendelman, H.E., Ikezu, T., 2010. CNS expression of anti-inflammatory cytokine interleukin-4 attenuates Alzheimer's disease-like pathogenesis in APP+PS1 bigenic mice. FASEB J. 24 (8), 3093–3102. https://doi.org/10.1096/fsb2.v24.810.1096/fj.10-155317.

Klempin, F., Kempermann, G., 2007. Adult hippocampal neurogenesis and aging. Eur. Arch. Psychiatry Clin. Neurosci. 257 (5), 271–280. https://doi.org/10.1007/s00406-007-0731-5.

Kokaia, Z., Martino, G., Schwartz, M., Lindvall, O., 2012. Cross-talk between neural stem cells and immune cells: the key to better brain repair? Nat. Neurosci. 15 (8), 1078–1087. https://doi.org/10.1038/nn.3163.

Koo, J.W., Duman, R.S., 2008. IL-1beta is an essential mediator of the antineurogenic and anhedonic effects of stress. Proc. Natl. Acad. Sci. U.S.A. 105 (2), 751–756. https://doi.org/10.1073/pnas.0708092105.

Kuhn, H.G., Dickinson-Anson, H., Gage, F.H., 1996. Neurogenesis in the dentate gyrus of the adult rat: age-related decrease of neuronal progenitor proliferation. J. Neurosci. 16 (6), 2027–2033. https://doi.org/10.1523/JNEUROSCI.16-06-02027.1996.

Kuipers, S.D., Schroeder, J.E., Trentani, A., 2015. Changes in hippocampal neurogenesis throughout early development. Neurobiol. Aging 36 (1), 365–379. https://doi.org/10.1016/j.neurobiolaging.2014.07.033.

Lavin, Y., Winter, D., Blecher-Gonen, R., David, E., Keren-Shaul, H., Merad, M., Jung, S., Amit, I., 2014. Tissue-resident macrophage enhancer landscapes are shaped by the local microenvironment. Cell 159 (6), 1312–1326. https://doi.org/10.1016/j.cell.2014.11.018.

Lazic, S.E., Fuss, J., Gass, P., Burne, T.H.J., 2014. Quantifying the behavioural relevance of hippocampal neurogenesis. PLoS ONE 9 (11), e113855. https://doi.org/10.1371/journal.pone.0113855.

Lee, J., Duan, W., Mattson, M.P., 2002. Evidence that brain-derived neurotrophic factor is required for basal neurogenesis and mediates, in part, the enhancement of neurogenesis by dietary restriction in the hippocampus of adult mice. J. Neurochem. 82 (6), 1367–1375. https://doi.org/10.1046/j.1471-4159.2002.01085.x.

Lichtenwalner, R.J., Forbes, M.E., Bennett, S.A., Lynch, C.D., Sonntag, W.E., Riddle, D.R., 2001. Intracerebroventricular infusion of insulin-like growth factor-I ameliorates the age-related decline in hippocampal neurogenesis. Neuroscience 107 (4), 603–613. https://doi.org/10.1016/s0306-4522(01)00378-5.

Linnartz, B., Neumann, H., 2013. Microglial activatory (immunoreceptor tyrosine-based activation motif)- and inhibitory (immunoreceptor tyrosine-based inhibition motif)-signaling receptors for recognition of the neuronal glycocalyx. Glia 61 (1), 37–46. https://doi.org/10.1002/glia.22359.

Lobo-Silva, D., Carriche, G.M., Castro, A.G., Roque, S., Saraiva, M., 2016. Balancing the immune response in the brain: IL-10 and its regulation. J Neuroinflammation. 13 (1), 297. https://doi.org/10.1186/s12974-016-0763-8.

Lucin, K.M., Wyss-Coray, T., 2009. Immune activation in brain aging and neurodegeneration: too much or too little? Neuron 64 (1), 110–122. https://doi.org/10.1016/j.neuron.2009.08.039.

Lyons, A., Downer, E.J., Crotty, S., Nolan, Y.M., Mills, K.H., Lynch, M.A., 2007. CD200 ligand receptor interaction modulates microglial activation in vivo and in vitro: a role for IL-4. J. Neurosci. 27 (31), 8309–8313. https://doi.org/10.1523/JNEUROSCI.1781-07.2007.

Lyons, A., Lynch, A.M., Downer, E.J., Hanley, R., O'Sullivan, J.B., Smith, A., Lynch, M.A., 2009. Fractalkine-induced activation of the phosphatidylinositol-3 kinase pathway attentuates microglial activation in vivo and in vitro. J. Neurochem. 110 (5), 1547–1556. https://doi.org/10.1111/j.1471-4159.2009.06253.x.

Manich, G., Recasens, M., Valente, T., Almolda, B., González, B., Castellano, B., 2019. Role of the CD200-CD200R axis during homeostasis and neuroinflammation. Neuroscience 405, 118–136. https://doi.org/10.1016/j.neuroscience.2018.10.030.

Mattson, M.P., Magnus, T., 2006. Ageing and neuronal vulnerability. Nat. Rev. Neurosci. 7 (4), 278–294. https://doi.org/10.1038/nrn1886.

Ming, G.-l., Song, H., 2005. Adult neurogenesis in the mammalian central nervous system. Annu. Rev. Neurosci. 28 (1), 223–250. https://doi.org/10.1146/annurev.neuro.28.051804.101459.

Mira, H., Morante, J., 2020. Neurogenesis from embryo to adult – lessons from flies and mice. Front. Cell Dev. Biol. 8, 533. https://doi.org/10.3389/fcell.2020.00533.

Monje, M.L., Toda, H., Palmer, T.D., 2003. Inflammatory blockade restores adult hippocampal neurogenesis. Science 302 (5651), 1760–1765. https://doi.org/10.1126/science.1088417.

Nakanishi, M., Niidome, T., Matsuda, S., Akaike, A., Kihara, T., Sugimoto, H., 2007. Microglia-derived interleukin-6 and leukaemia inhibitory factor promote astrocytic differentiation of neural stem/progenitor cells. Eur. J. Neurosci. 25 (3), 649–658. https://doi.org/10.1111/j.1460-9568.2007.05309.x.

Nakanishi, H., Wu, Z., 2009. Microglia-aging: roles of microglial lysosome- and mitochondria-derived reactive oxygen species in brain aging. Behav. Brain Res. 201 (1), 1–7. https://doi.org/10.1016/j.bbr.2009.02.001.

Ojo, J.O., Rezaie, P., Gabbott, P.L., Stewart, M.G., 2015. Impact of age-related neuroglial cell responses on hippocampal deterioration. Front. Aging Neurosci. 7, 57. https://doi.org/10.3389/fnagi.2015.00057.

Packer, M.A., Stasiv, Y., Benraiss, A., Chmielnicki, E., Grinberg, A., Westphal, H., Goldman, S.A., Enikolopov, G., 2003. Nitric oxide negatively regulates mammalian adult neurogenesis. Proc Natl Acad Sci U S A. 100 (16), 9566–9571. https://doi.org/10.1073/pnas.1633579100.

Palmer, T.D., Willhoite, A.R., Gage, F.H., 2000. Vascular niche for adult hippocampal neurogenesis. J. Comp. Neurol. 425 (4), 479–494. https://doi.org/10.1002/1096-9861(20001002)425:4<479::aid-cne2>3.0.co;2-3.

Pawley, L.C., Hueston, C.M., O'Leary, J.D., Kozareva, D.A., Cryan, J.F., O'Leary, O.F., Nolan, Y.M., 2020. Chronic intrahippocampal interleukin-1β overexpression in adolescence impairs hippocampal neurogenesis but not neurogenesis-associated cognition. Brain Behav. Immun. 83, 172–179. https://doi.org/10.1016/j.bbi.2019.10.007.

Pereira, L., Font-Nieves, M., Van den Haute, C., Baekelandt, V., Planas, A.M., Pozas, E., 2015. IL-10 regulates adult neurogenesis by modulating ERK and STAT3 activity. Front. Cell. Neurosci. 9, 57. https://doi.org/10.3389/fncel.2015.00057.

Perez-Asensio, F.J., Perpiñá, U., Planas, A.M., Pozas, E., 2013. Interleukin-10 regulates progenitor differentiation and modulates neurogenesis in adult brain. J. Cell Sci. 126 (Pt 18), 4208–4219. https://doi.org/10.1242/jcs.127803.

Recasens, M., Shrivastava, K., Almolda, B., González, B., Castellano, B., 2019. Astrocyte-targeted IL-10 production decreases proliferation and induces a downregulation of activated microglia/macrophages after PPT. Glia. 67 (4), 741–758. https://doi.org/10.1002/glia.23573.

Reshef, R., Kudryavitskaya, E., Shani-Narkiss, H., Isaacson, B., Rimmerman, N., Mizrahi, A., Yirmiya, R., 2017. The role of microglia and their CX3CR1 signaling in adult neurogenesis in the olfactory bulb. Elife. 6, e30809. https://doi.org/10.7554/eLife.30809.

Revest, J.M., Dupret, D., Koehl, M., Funk-Reiter, C., Grosjean, N., Piazza, P.V., Abrous, D. N., 2009. Adult hippocampal neurogenesis is involved in anxiety-related behaviors. Mol. Psychiatry 14 (10), 959–967. https://doi.org/10.1038/mp.2009.15.

Ryan, S.M., O'Keeffe, G.W., O'Connor, C., Keeshan, K., Nolan, Y.M., 2013. Negative regulation of TLX by IL-1β correlates with an inhibition of adult hippocampal neural precursor cell proliferation. Brain Behav. Immun. 33, 7–13. https://doi.org/10.1016/j.bbi.2013.03.005.

Sanchez-Molina, P., Almolda, B., Benseny-Cases, N., González, B., Perálvarez-Marín, A., Castellano, B., 2021. Specific microglial phagocytic phenotype and decrease of lipid oxidation in white matter areas during aging: implications of different microenvironments. Neurobiol. Aging 105, 280–295. https://doi.org/10.1016/j.neurobiolaging.2021.03.015.

Saxe, M.D., Battaglia, F., Wang, J.W., Malleret, G., David, D.J., Monckton, J.E., Garcia, A. D., Sofroniew, M.V., Kandel, E.R., Santarelli, L., Hen, R., Drew, M.R., 2006. Ablation of hippocampal neurogenesis impairs contextual fear conditioning and synaptic plasticity in the dentate gyrus. Proc. Natl. Acad. Sci. U.S.A. 103 (46), 17501–17506. https://doi.org/10.1073/pnas.0607207103.

Saxton, R.A., Tsutsumi, N., Su, L.L., Abhiraman, G.C., Mohan, K., Henneberg, L.T., Aduri, N.G., Gati, C., Garcia, K.C., 2021. Structure-based decoupling of the pro- and anti-inflammatory functions of interleukin-10. Science 371 (6535), eabc8433. https://doi.org/10.1126/science.abc8433.

Scharfman, H., Goodman, J., Macleod, A., Phani, S., Antonelli, C., Croll, S., 2005. Increased neurogenesis and the ectopic granule cells after intrahippocampal BDNF infusion in adult rats. Exp. Neurol. 192 (2), 348–356. https://doi.org/10.1016/j.expneurol.2004.11.016.

Sheng, W.S., Hu, S., Ni, H.T., Rowen, T.N., Lokensgard, J.R., Peterson, P.K., 2005. TNF-alpha-induced chemokine production and apoptosis in human neural precursor cells. J. Leukoc. Biol. 78 (6), 1233–1241. https://doi.org/10.1189/jlb.0405221.

Sierra, A., Encinas, J.M., Deudero, J.J., Chancey, J.H., Enikolopov, G., Overstreet-Wadiche, L.S., Tsirka, S.E., Maletic-Savatic, M., 2010. Microglia shape adult hippocampal neurogenesis through apoptosis-coupled phagocytosis. Cell Stem Cell 7 (4), 483–495. https://doi.org/10.1016/j.stem.2010.08.014.

Sierra, A., Gottfried-Blackmore, A.C., McEwen, B.S., Bulloch, K., 2007. Microglia derived from aging mice exhibit an altered inflammatory profile. Glia 55 (4), 412–424. https://doi.org/10.1002/glia.20468.

Snyder, J.S., Hong, N.S., McDonald, R.J., Wojtowicz, J.M., 2005. A role for adult neurogenesis in spatial long-term memory. Neuroscience 130 (4), 843–852. https://doi.org/10.1016/j.neuroscience.2004.10.009.

Stanfield, B.B., Trice, J.E., 1988. Evidence that granule cells generated in the dentate gyrus of adult rats extend axonal projections. Exp. Brain Res. 72 (2), 399–406. https://doi.org/10.1007/BF00250261.

Taliaz, D., Stall, N., Dar, D.E., Zangen, A., 2010. Knockdown of brain-derived neurotrophic factor in specific brain sites precipitates behaviors associated with depression and reduces neurogenesis. Mol. Psychiatry 15 (1), 80–92. https://doi.org/10.1038/mp.2009.67.

Taupin, P., Gage, F.H., 2002. Adult neurogenesis and neural stem cells of the central nervous system in mammals. J. Neurosci. Res. 69 (6), 745–749. https://doi.org/10.1002/jnr.10378.

Udeochu, J.C., Shea, J.M., Villeda, S.A., 2016. Microglia communication: Parallels between aging and Alzheimer's disease. Clin. Exp. Neuroimmunol. 7 (2), 114–125. https://doi.org/10.1111/cen3.2016.7.issue-210.1111/cen3.12307.

Vallières, L., Campbell, I.L., Gage, F.H., Sawchenko, P.E., 2002. Reduced hippocampal neurogenesis in adult transgenic mice with chronic astrocytic production of interleukin-6. J. Neurosci. 22 (2), 486–492. https://doi.org/10.1523/JNEUROSCI.22-02-00486.2002.

van Praag, H., Shubert, T., Zhao, C., Gage, F.H., 2005. Exercise enhances learning and hippocampal neurogenesis in aged mice. J. Neurosci. 25 (38), 8680–8685. https://doi.org/10.1523/JNEUROSCI.1731-05.2005.

Varnum, M.M., Kiyota, T., Ingraham, K.L., Ikezu, S., Ikezu, T., 2015. The anti-inflammatory glycoprotein, CD200, restores neurogenesis and enhances amyloid phagocytosis in a mouse model of Alzheimer's disease. Neurobiol. Aging 36 (11), 2995–3007. https://doi.org/10.1016/j.neurobiolaging.2015.07.027.

Villeda, S.A., Luo, J., Mosher, K.I., Zou, B., Britschgi, M., Bieri, G., Stan, T.M., Fainberg, N., Ding, Z., Eggel, A., Lucin, K.M., Czirr, E., Park, J.S., Couillard-Després, S., Aigner, L., Li, G., Peskind, E.R., Kaye, J.A., Quinn, J.F., Galasko, D.R., Xie, X.S., Rando, T.A., Wyss-Coray, T., 2011. The ageing systemic milieu negatively regulates neurogenesis and cognitive function. Nature 477 (7362), 90–94. https://doi.org/10.1038/nature10357.

Vukovic, J., Colditz, M.J., Blackmore, D.G., Ruitenberg, M.J., Bartlett, P.F., 2012. Microglia modulate hippocampal neural precursor activity in response to exercise and aging. J. Neurosci. 32 (19), 6435–6443. https://doi.org/10.1523/JNEUROSCI.5925-11.2012.

Wagner, J.P., Black, I.B., DiCicco-Bloom, E., 1999. Stimulation of neonatal and adult brain neurogenesis by subcutaneous injection of basic fibroblast growth factor. J. Neurosci. 19 (14), 6006–6016. https://doi.org/10.1523/JNEUROSCI.19-14-06006.1999.

Wolf, S.A., Steiner, B., Akpinarli, A., Kammertoens, T., Nassenstein, C., Braun, A., Blankenstein, T., Kempermann, G., 2009. CD4-positive T lymphocytes provide a neuroimmunological link in the control of adult hippocampal neurogenesis. J. Immunol. 182 (7), 3979–3984. https://doi.org/10.4049/jimmunol.0801218.

Wynne, A.M., Henry, C.J., Huang, Y., Cleland, A., Godbout, J.P., 2010. Protracted downregulation of CX3CR1 on microglia of aged mice after lipopolysaccharide challenge. Brain Behav. Immun. 24 (7), 1190–1201. https://doi.org/10.1016/j.bbi.2010.05.011.

Zigova, T., Pencea, V., Wiegand, S.J., Luskin, M.B., 1998. Intraventricular administration of BDNF increases the number of newly generated neurons in the adult olfactory bulb. Mol. Cell. Neurosci. 11 (4), 234–245. https://doi.org/10.1006/mcne.1998.0684.

Ziv, Y., Schwartz, M., 2008. Immune-based regulation of adult neurogenesis: implications for learning and memory. Brain Behav. Immun. 22 (2), 167–176. https://doi.org/10.1016/j.bbi.2007.08.006.